RESEARCH INSTITUTE FOR TECHNICAL PHYSICS

OF THE HUNGARIAN ACADEMY OF SCIENCES

A MAGYAR TUDOMÁNYOS AKADÉMIA MŰSZAKI

FIZIKAI KUTATÓINTÉZETÉNEK

COMMUNIQUÉ

KÖZLEMÉNYEI

0 – 6

623981

SOME ASPECTS OF SPECTROMETRY
By: J. Schanda

ELECTROSTATIC ENERGY IN ABRUPT SEMICONDUCTOR HETEROJUNCTION
By: I. Markó.

ON THE MINORITY CARRIER LIFETIME ANISOTROPY IN PLASTICALLY DEFORMED P–TYPE GERMANIUM
By: I. Cseh and B. Pődör.

MTA
KIK

476143

MAGYAR
TUDOMÁNYOS AKADÉMIA
KÖNYVTÁRA

ИНСТИТУТ ТЕХНИЧЕСКОЙ ФИЗИКИ
ВЕНГЕРСКОЙ АКАДЕМИИ НАУК

RESEARCH INSTITUTE FOR TECHNICAL PHYSICS
OF THE HUNGARIAN ACADEMY OF SCIENCES
Budapest, Ujpest 1.Pf. 76.

Felelős kiadó: Szigeti György akadémikus, igazgató
Müszaki szerkesztő: Gomperz Istvánné

73-351 "TEMPÓ" 200 pld.
Felelős vezető: Szerencsi Sándor

R 1977

M. TUD. AKADÉMIA KÖNYVTÁRA
Könyvtelt 5410 /1973 sz.

SOME ASPECTS OF SPECTRORADIOMETRY

Contents

o o o

1. Introduction

The aim of the present paper is not to give a comprehensive treatise of all the questions of spectral power distribution measurements, but only to sum up the most important basic laws and relations of measuring optical power, and then to deal with some problems influencing the accuracy of spectroradiometry.

In the following our attention will be directed towards the wavelength range of the electromagnetic spectrum seen in Fig. 1. Here the usual notations of the single spectral bands can

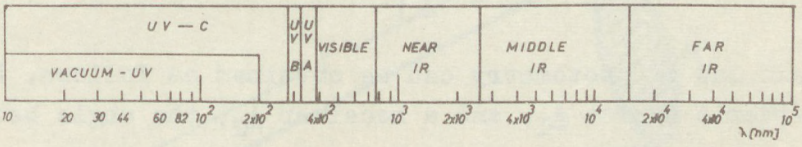

Fig. 1
The electromagnetic spectrum

be read as well. The vacuum-ultraviolet, middle, and far infrared parts of the spectrum, although of outstanding importance, will not be discussed in this paper, as their measurement technical aspects /power sources, construction of wavelength resolving instruments, detectors/ differ considerably from those of the visible and classical ultraviolet radiation onto which our primary interest is focused on.

In the following first the most important radiometric quantities and relations will be reconsidered. This will be followed

by the discussion of questions related to different radiation sources, monochromators /band-width problems/, detectors of radiation /the problem of information extraction from noisy signals/ and spectrometer systems.

2. Basic laws and relations of radiated power

The basic difference between optical /and photometric/ measurements and the usual physical and chemical measurements related to the flux of energy is that here we have to deal with radiation propagating along straight lines. There is always a propagation of the radiation from the source within a given cone, determined by the optical system.

Taking the quantity of radiant energy /Q/ as the initial quantity the radiant flux /or radiant power/ is reached as

$$P = \frac{d\,Q}{d\,t} \qquad 1$$

The basic law of photometry can be obtained as follows. Let us consider a source A_1, and a receiver A_2, the angle between

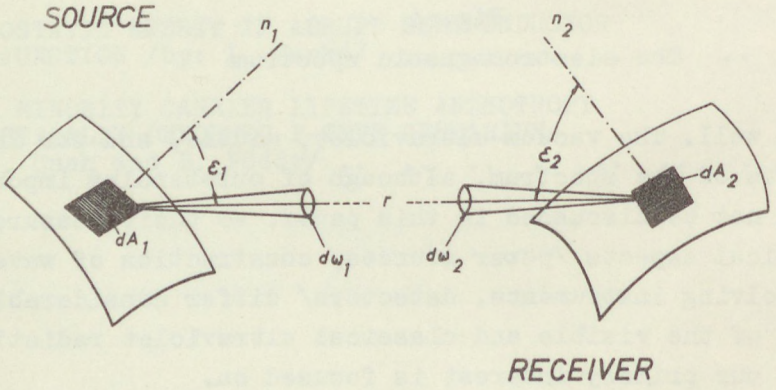

Fig. 2
Illustration to the basic law of photometry

the normals of these surfaces and the direction joining them is marked by ε_1 and ε_2, resp., their distance by r /see Fig. 2/.

And now the specially optical quantity: The radiant power emitted by A_1 in a given direction can be regarded as emitted in a given solid angle, thus some kind of density for the solid angle is constructed: The radiant intensity I /principally defined for a point source/ reflects the fact that the radiant power is distributed within a finite solid angle:

$$I(\varepsilon) = \frac{d P(\varepsilon)}{d \omega} \qquad 2$$

where $\omega = \frac{A}{r^2}\Omega$ /the meaning of the single quantities is shown in Fig. 3/.

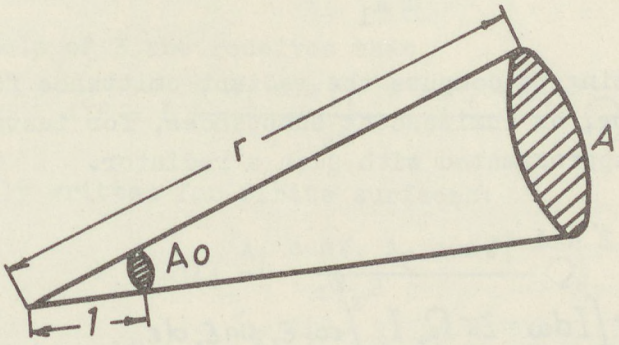

Fig. 3
The distribution of radiant power within a finite solid angle

In case of extended sources it is usual to define the density of the radiant flux within the solid angle around the direction of emission for the unity of projected area of the source, this is the radiance:

$$L = \frac{d I}{dA_1 \cos\varepsilon_1} = \frac{d^2 P}{d\omega\, dA_1 \cos\varepsilon_1} \qquad 3$$

In the special case when $\underline{I}$ is proportional to the cosine of the angle ε_1 and is independent of the azimuth angle, $\underline{L}$ becomes independent of the direction of emission: If

$$I = I_o \cos \varepsilon_1$$

$$\text{than} \quad L = \frac{1}{A_1 \cos \varepsilon_1} = \frac{I_o}{A_1} \qquad 4$$

where $\underline{I}_o$ is the radiant intensity in the direction of the normal of the surface.

This relation expresses the so-called Lambert's law.

Sometimes the radiant emittance, the total emitted flux /within the solid angle of the half sphere: $\omega = 2\pi$ sr/ of a given surface is also of interest:

$$M = \frac{d P}{d A_1} \qquad 5$$

(It is interesting to compute the radiant emittance for a Lambertion radiator, as luminescent substances, for instance, can often be well approximated with such a radiator.

By the help of 2 and 4:

$$P = \int_0 \frac{dP}{d\omega} d\omega = \int_0 I \, d\omega = 2\pi \Omega_o I_o \int_0^{\pi/2} \cos \varepsilon_1 \sin \varepsilon_1 \, d\varepsilon_1$$

because

$$d\omega = 2\pi \Omega_o \sin \varepsilon_1 \, d\varepsilon_1$$

and thus $P = \pi I_o \Omega_o$

and $M = \frac{P}{f_1} = \pi \Omega_o \frac{I_o}{A_1} = \pi \Omega_o L$)

The radiant flux travels through the optical instrument and at the end reaches the receptor. This might be a photon-detector, a luminescent material or a sample where the radiation has to perform some biological or chemical change, or only a

surface acting as a secondary source. For these the radiant power striking the surface element, called the irradiation, is the pertinent measure and is defined as

$$E = \frac{d P}{d A_2} \qquad 6$$

Let us now investigate the quantity of radiation sent from surface element d A_1 to surface element d A_2 /see Fig. 2/:

According to 2

$$d^2 P(\varepsilon) = d I(\varepsilon)\, d\omega$$

From Fig. 2 and 3 it is seen that

$$d\omega = \frac{dA_2 \cos\varepsilon_2}{r^2}\,\Omega_o$$

So that

$$d^2P = dI(\varepsilon_1)\frac{d A_2 \cos\varepsilon_2}{r^2}\,\Omega_o$$

and by the help of 3 one receives that

$$d^2P = L\,\frac{d A_1 \cos\varepsilon_1 \; d A_2 \cos\varepsilon_2}{r^2}\,\Omega_o$$

or, as usually written for finite surfaces:

$$P = L(\varepsilon_1)\,\frac{A_1 \cos\varepsilon_1 \; A_2 \cos\varepsilon_2}{r^2}\,\Omega_o \qquad 7$$

This relation is called the basic principle of photometry. Here also the special character of a Lambertian radiator is seen, as for this L is independent of ε_1, and thus P, the radiant flux at A_2 depends only on the projected area of the two surfaces and their distance.

Table 1 summarizes the basic radiometric concepts and their units. /In the present paper, for sake of simplicity, we omitted the indices e, defining the radiometric quantities. It is usual to denote the radiometric quantities by the index e, and the corresponding photometric ones without an index. /The lat-

Basic Radiometric Concepts and Units — Table 1.

Term	Symbol	Defining Equation	Explanatory Notes and Formulas		Units
Radiant energy					erg
Radiant flux	P			$d^2P = L \frac{dA_1 \cos\varepsilon_1 \, dA_2 \cos\varepsilon_2}{r^2}$	erg s^{-1}
Radiant emittance	M	$M = \frac{dP}{dA_1}$	dA_1: surface element of source	= flux from source element dA_1 incident on receiver element dA_2	erg s^{-1} cm^{-2}
Irradiance	E	$E = \frac{dP}{dA_2}$	dA_2: surface element of receiver		erg s^{-1} cm^{-2}
Radiant intensity	I	$I = \frac{dP}{d\omega_1}$	$d\omega_1$: element of solid angle with apex /1/ at surface of source		erg s^{-1} sr^{-1}
Radiance	L	$L = \frac{d^2P}{dA_1 \cos\varepsilon_1 \, d\omega_1}$	ε_1: angle between given direction /1/-/2/ and normal n_1 of dA_1	$dA_1 \cos\varepsilon_1$: dA_1 orthogonally projected on plane perpendicular to given direction /1/-/2/	erg s^{-1} cm^{-2} sr^{-1}
		$= \frac{d^2E}{dA_2 \cos\varepsilon_2 \, d\omega_2}$	ε_2: angle between given direction /1/-/2/ and normal n_2 of dA_2	$dA_2 \cos\varepsilon_2$: dA_2 orthogonally projected on plane perpendicular to given direction /1/-/2/	
		$= \frac{d(E)}{d\omega_2}$	$d\omega_2$: element of solid angle with apex /2/ at surface of receiver	$d(E)_2 = \frac{dE}{dA_2 \cos\varepsilon_2}$	
Solid angle	ω	$\omega = \frac{S}{r}$	S : portion of sphere surface	$d\omega_1 = \frac{dA_2 \cos\varepsilon_2}{r^2}$	sr /steradian/
			r : radius of sphere, also distance between /1/ of dA_1 and /2/ of dA_2	$d\omega_2 = \frac{dA_1 \cos\varepsilon_1}{r^2}$	
Frequency	ν				s^{-1}
Wavelength	λ	$\lambda = c/\nu$	c : velocity of radiant energy in vacuo		cm
Wavenumber	ν'	$\nu' = \nu/c$			cm^{-1}

ter can be constructed from the radiometric ones by integrating the product of the radiometric quantity and the relative photopic luminous efficiency function ($\underline{V}(\lambda)$) over the visible wavelength range and by multiplying this with the value of the maximum luminous efficacy $\underline{K}_m = 680$ lum/W , thus e.g. the luminous intensity is gained from the radiant intensity in the following way:

$$I = K_m \int_{380}^{780} I_{e\lambda} V(\lambda) \, d\lambda \qquad 8$$

However, the photometric quantities will be used in this paper only in those few cases, where the sensitivity of radiation detectors is defined in photometric units. Otherwise we will keep us to the radiometric units and will designate them without the index e.

3. Further quantities

3.1 Spectral quantities

All the basic quantities discussed in the preceding section are, naturally, wavelength dependent. As finite energy can propagate only in a finite wavelength range, it is usual to define the spectral /monochromatic/ quantities as distribution functions, i.e. to put the wavelength derivative curves, generally visualized by a λ index, so that the radiometric quantities are received as the product of the distribution function and the wavelength interval. Thus, e.g.

$$P_\lambda = \frac{d\,P(\lambda)}{d\,\lambda} , \quad \text{and} \quad \Delta P(\lambda) = \frac{d\,P(\lambda)}{d\,\lambda} \Delta\lambda \qquad 9$$

It is worth mentioning that it is usual to use different units for given radiometric quantities. E.g. the radiance and irradiance can be measured as

$$L \left[\frac{W}{cm^2\ sr} \right] \quad \text{and} \quad E \left[\frac{W}{cm^2} \right]$$

/in the first one cm^2 refers to the area of the source, in the second to that of the receiver!/ and the spectral distribution function of these as

$$L_\lambda \left[\frac{W}{cm^2 nm\ sr} \right] \quad \text{and} \quad E_\lambda \left[\frac{W}{cm^2 nm} \right]$$

but also as

$$L_\lambda \left[\frac{W}{cm^3\ sr} \right] \quad \text{and} \quad E_\lambda \left[\frac{W}{cm^3} \right] \qquad 10$$

or even very often as the distribution for a 10 nm interval.

Quite often the absolute value of the spectral distribution functions is of minor importance, and it is sufficient to calculate the relative distributions. This might lead to a considerable simplification in measurement techniques. In such cases the

$$\left(P_\lambda \right)_{rel} = \frac{P_\lambda}{P_\lambda (\lambda_o)} \qquad 11$$

function is used, and as the numerical values of all the relative distribution functions are the same, it is usual to speak quite generally about the relative spectral distribution function E_λ, independently whether it is a radiant flux, an irradiation, radiance, or something else. The dimensions become important only if the absolute value of the particular function at the reference wavelength is given, too.

In physical, chemical and biologival measurements it is often more convenient to work with wavenumber or electron energy /frequency/ as independent variables. In this connection it has to be pointed out that not only the scale but also the shape of the distribution curves /for instance also the place of the maximum of a curve/ change by using instead of wavelength dependent functions frequency dependent ones. This change is due to the fact that the distribution functions define the variable for the unity of the

independent variable, thus the power itself has to remain unchanged independent of its measure:

$$E_\nu \, d\nu = E_\lambda \, d\lambda \qquad 12$$

As well-known

$$\nu = c/\lambda$$

and thus

$$d\nu = -\frac{c}{\lambda^2} d\lambda \qquad 13$$

Substituting this into 12 we obtain

$$\underline{\underline{E_\nu}} = -\frac{\lambda^2}{c} E_\lambda \sim \underline{\underline{-\lambda^2 E_\lambda}} \qquad 14$$

For the relative distributions this means the following: the negative sign shows that the direction of scaling is opposite, and one gets from the wavelength dependent spectral distribution the frequency /wavenumber, photon energy/ dependent one by multiplying the E_λ function by the square of the wavelength.

To reach the relative distributions in numbers of photons within a photon energy interval a further multiplication with wavelength is necessary, as

$$E_\nu \, d\nu = \frac{N}{t} h\nu \, d\nu \qquad 15$$

3.2 Temperature definitions

The temperature of an incandescent light source and the correlated colour temperature of a selective radiator belong to the most basic quantities of these sources. Therefore some further definitions have to be introduced. As well-known the only radiator the spectral distribution of which can be calculated is the black-body radiator. /See also Sec. 4.1.2./ A practical temperature radiator can be defined by its real temperature and its /wavelength dependent/ emissivity $\varepsilon(\lambda, T)$. For such a radiator the ra-

diant emittance, for instance, is received in the following way:

$$M^{*}_{\lambda}(T) = \varepsilon(\lambda, T)\ M_{\lambda}(T) \qquad 16$$

A radiator is called gray, if its emissivity is smaller than unity, but constant in the wavelength range under consideration.

Most of the practical sources show, however, a wavelength dependent emissivity. If the emissivity shows an inverse exponential wavelength dependence in a given spectral range, a distribution temperature of the source can be defined. This is the absolute temperature (in K) of the blackbody radiator for which the spectral energy distribution, at every wavelength of the given spectral range /usually the visible spectrum/ is /approximately/ proportional to that of the source considered.

Another term, often mixed up with distribution temperature is that of colour temperature. In this case the light of the considered radiator should have /nearly/ the same chromaticity coordinates as a blackbody radiator at a certain temperature called colour temperature.

We only mention here that for radiators, the colour of which differs more considerably from that of a blackbody, the term correlated colour temperature has been coined, it is the temperature of a blackbody radiator with the nearest chromaticity match.

A frequently used term for temperature radiators is the luminance temperature. It is the absolute temperature of a blackbody radiator for which the luminance at a specified wavelength has the same spectral concentration as for the radiator considered. In practice the reference wavelength is generally 655 nm.

4. Radiation sources

The different types of radiation sources will be discussed from the following practical point of view: Sources used as standards and excitation sources.

4.1 Standard sources

4.1.1 Wavelength standards

The first problem in every spectrometric measurement is the wavelength calibration of the monochromator. For this purpose usually spectral-lamps, gas discharge lamps with a metal and/or noble gas filling are used. Attention has to be paid in using these lamps in so far as they are gas-discharge tubes, thus posess negative characteristics, the nominal current has to be set by the help of a controlable ballast. Deviations from the nominal current influence the emission: at higher current levels the spectral lines broaden up, even self-absorption might occur. At smaller currents the lines become sharper but the lamp deteroriates rapidly as the electrode temperature is not enough for producing the necessary electron-concentration. In case of metal gas-discharges there is always a noble gas filling present to start the lamp. Some noble gas spectral lines are emitted even after the lamp has started; and as manufacturers usually do not state what type of filling they use, these unknown lines can often produce some confusion. Therefore it can be only suggested to take spectrographic pictures of the spectral lamps and to use the so prepared "spectral atlas" in calibrating the instruments. Table 2 contains some of the most popular spectral lamps of the factories Osram and Philips.

Table 2

Spectral lamps and their manufacturer

Filling	Burner Loading		
	Osram		Philips
	[W]	[A]	[W]
Argon			15
Caesium	20	1.5	10
Cadmium	18		25
Helium	65	1.3	45
Krypton	15		
Mercury	30; 56	1.0; 1.2	15; 90
Neon	40	1.5	25
Potassium	14	1.5	20
Rubidium	13	1.5	15
Sodium	25	1.3	15
Thallium	13	1.0	
Xenon			10
Zink	20	1,5	25

4.1.2 Radiation standards

The principle standard of optical radiation is, as well-known, the blackbody radiator, as this is the only radiator whose spectral distribution can be calculated theoretically. The theoretical basis of Planck's law and the practical realizations of blackbody sources is discussed in standard text and reference books, thus here we will not deal with these questions in detail. From our practical point of view it is enough to register that the blackbody radiator is our primary standard, and that for this Planck's formula describing the spectral radiant emittance is valid:

$$M_\lambda = 2\pi hc^2 \lambda^{-5} \left[\exp(hc/kT\lambda) - 1\right]^{-1} \qquad 17$$

At the present accepted values of the two radiation constants are the following:[2]

$$c_1 = 2\pi hc^2 = 3{,}7415 \cdot 10^{-16}\ \mathrm{Wm}^2$$

$$c_2 = \frac{h\,c}{k} = 1{,}43879 \cdot 10^{-2}\ \mathrm{mK} \qquad 18$$

The first constant changes only the absolute value of the emitted radiation, thus it has no importance in relative spectral distribution measurements. This is, however, not the case for the second constant, where a change from $\underline{c}_2$ to $\underline{c}_2' = \underline{a}\ \underline{c}_2$ influences a change in temperature: a tabulation of Planck's distribution valid in case of $\underline{c}_2$ for the temperature T, will be valid for $\underline{c}_2'$ for a temperature $\underline{T}' = \underline{a}$ T. In the field of spectrometry usually the value adopted by the CIE /International Commission on Illumination/:[3]

$$c_2 = 1{,}4380 \cdot 10^{-2}\ \mathrm{mK} \qquad 19$$

is used.

It has to be kept in mind that this determination uncertainty of the $\underline{c}_2$ constant presents an ultimate limit in spectrometric accuracy.

For practical purposes secondary standards are used. For decades the tungsten ribbon lamp served as secondary standard, nowadays quartz-halogen lamps become increasingly popular.

Tungsten ribbon lamps are usually available calibrated for luminance temperature and for determining their spectral power distribution first either their real temperature /than calculating according to Equ. 16./ or the distribution temperature belonging to the luminance

Table 3

Spectral Emissivity of Tungsten [4,5]

λ [nm]	Temperature /K/						
	1600	1800	2000	2200	2400	2600	2800
300	0,480	0,476	0,474	0,468	0,463	0,459	0,454
10	0,479	0,475	0,471	0,468	0,464	0,459	0,454
20	0,477	0,474	0,470	0,466	0,463	0,459	0,455
30	0,476	0,473	0,470	0,466	0,463	0,460	0,456
40	0,476	0,473	0,470	0,467	0,464	0,461	0,457
50	0,477	0,474	0,471	0,468	0,465	0,462	0,459
60	0,479	0,476	0,473	0,470	0,467	0,464	0,461
70	0,480	0,477	0,474	0,471	0,468	0,464	0,461
80	0,480	0,477	0,474	0,470	0,467	0,464	0,460
90	0,480	0,476	0,473	0,470	0,466	0,463	0,460
400	0,479	0,475	0,472	0,469	0,465	0,462	0,459
20	0,476	0,473	0,469	0,465	0,463	0,459	0,456
40	0,474	0,470	0,466	0,463	0,460	0,456	0,453
60	0,471	0,467	0,464	0,460	0,457	0,453	0,450
80	0,469	0,465	0,462	0,458	0,455	0,451	0,448
500	0,467	0,463	0,460	0,456	0,453	0,449	0,446
20	0,465	0,461	0,458	0,454	0,451	0,447	0,444
40	0,463	0,459	0,456	0,452	0,449	0,446	0,442
60	0,460	0,457	0,453	0,449	0,446	0,443	0,440
80	0,457	0,453	0,450	0,446	0,443	0,439	0,436
600	0,453	0,450	0,446	0,443	0,439	0,436	0,432
20	0,450	0,447	0,443	0,440	0,436	0,433	0,429
40	0,448	0,445	0,441	0,437	0,434	0,430	0,426
60	0,446	0,443	0,439	0,435	0,431	0,427	0,424
80	0,444	0,440	0,436	0,432	0,428	0,424	0,420
700	0,442	0,438	0,434	0,430	0,425	0,421	0,417
20	0,440	0,436	0,431	0,427	0,422	0,418	0,414
40	0,437	0,433	0,428	0,423	0,418	0,414	0,410
60	0,435	0,430	0,425	0,419	0,415	0,410	0,406
80	0,432	0,427	0,422	0,416	0,411	0,406	0,402
800	0,429	0,423	0,418	0,412	0,407	0,402	0,398

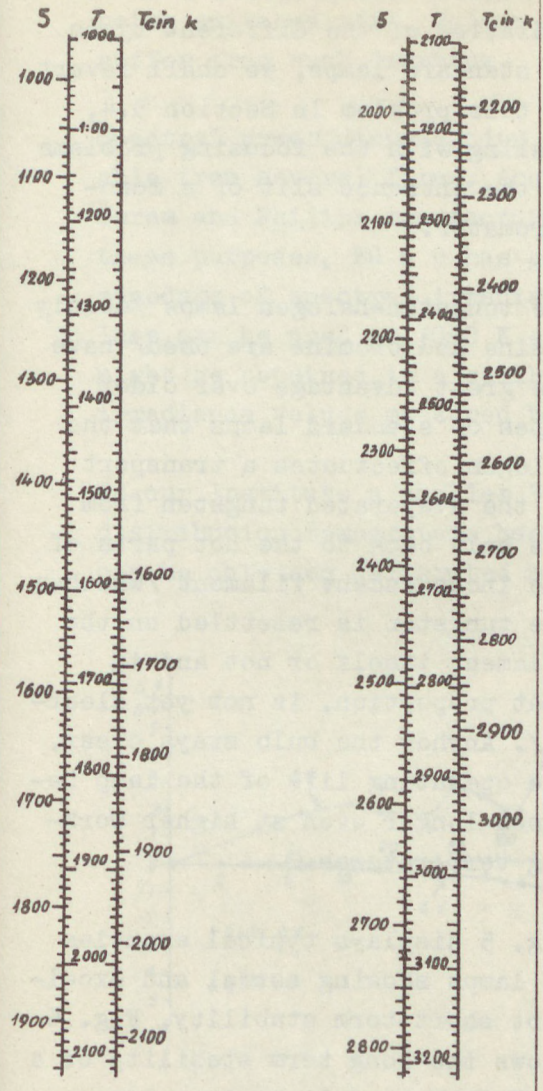

Fig. 4

Nomogram showing the correlation between true temperature /T/, luminance temperature /S/ and colour temperature /Tc/ [6]

temperature under consideration has to be determined. Table 3 contains de Vos's spectral emissivity data of tungsten, as corrected by Rutgers and Schurer. By the help of this and a blackbody radiation table the spectral power distribution of the lamp can be determined using Equ. 16. Fig. 4 shows a nomogram by the help of which the calculations between the different "temperatures" are made easier.

Tungsten coiled filament lamps emit a composed spectrum: The outer surface of the filament radiates as tungsten, the inner part of the coiles shows an emission lying nearer to that of a blackbody. For this reason it is usual to express the working characteristics of a coiled filament lamp by giving its distribution temperature. In this case the spectral power distribution can be directly determined from a blackbody table. [7]

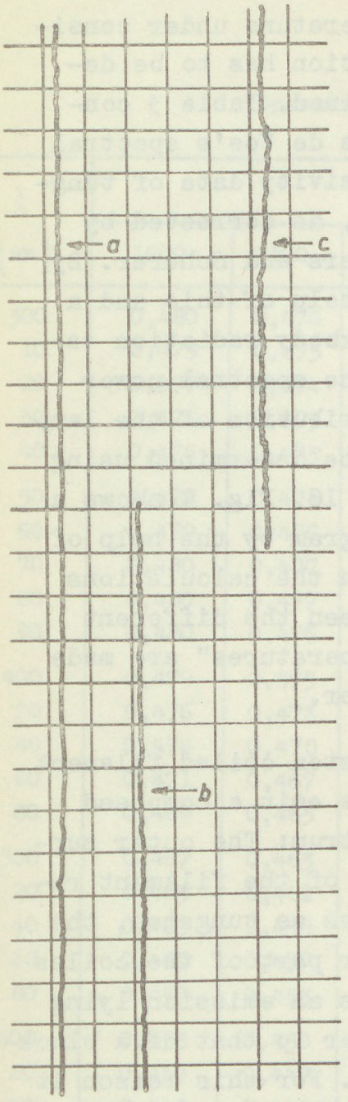

Fig. 5

Short term stability of three tungsten-halogen lamps

As regards the projection of the radiation of the different types of standard lamps, we shall revert to this problem in Section 5.4, dealing with the focusing problems at the entrance slit of a monochromator.

The tungsten-halogen lamps /mostly iodine and bromine are used/ have the great advantage over older types of standard lamps that the halogen effectuates a transport of the evaporated tungsten from the bulb back to the hot parts of the incandescent filament /whether the tungsten is resettled on the filament itself or not and in what proportion, is not yet cleared/. Anyhow the bulb stays clear, the operating life of the lamp becomes longer even at higher working temperatures.[8]

Fig. 5 displays typical examples of lamps showing normal and excellent short term stability, Fig. 6 shows the long term stability of a 12 V 55 W head light type lamp /Tungsram 50310 tip/ /type a in Fig. 5/ used underrated at approximately 10 V, providing a distribution temperature of 2854 K.[9]

Measurements showed that for the older tungsten-iodine lamps a shallow absorption band appears in the green region of the spectrum /these lamps show the character-

istic purple colour due to excess iodine vapour after being switched off/. Modern multi-halogen lamps do not suffer from such drawback.

Spectral power distribution standard lamps are available from several firms. According to our knowledge Osram and Philips manufacture tungsten ribbon lamps for these purposes, EG & G has a 1000 W quartz-halogen lamp standard of spectral irradiance on the market. This lamp can be used at 3060 K colour temperature, and might be obtained in a calibrated version with spectral irradiance values measured between 250 and 2500 nm.

In our Institute a smaller 50 W standard with 2854 K distribution temperature has been elaborated.This lamp can be obtained calibrated between 350 and 830 nm.

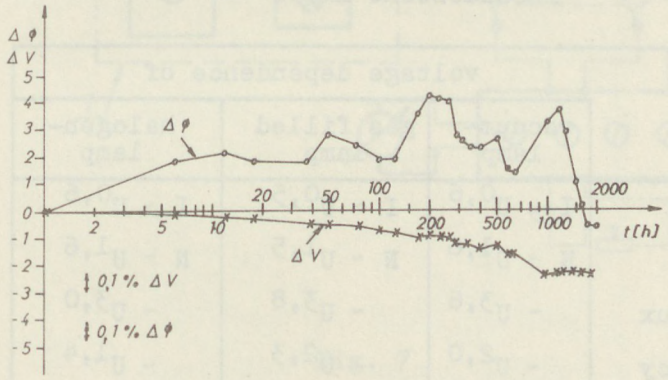

Fig. 6

Long term stability of a tungsten-halogen lamp
$\Delta\phi$ curve: Light flux changes; ΔV curve: Voltage changes in case of constant current supply

The voltage of the tungsten-halogen lamps cannot be set to any desired value, since if the voltage would be too law, the halogen cycle could not start /a bulb tempera-

ture of approx. 350 ~ 450°C is necessary/, if the voltage is too high an untimely burn-out would be the consequence.

Table 4 shows how the working characteristics of different types of incandescent lamps change with voltage. As seen the luminous flux changes as a high power of voltage. The spectral intensity, especially at the short wavelength end of the spectrum changes even more rapidly, thus as a rough estimate one can calculate with the following: the stability of the lamp current has to be maintained by an order of magnitude higher than that required for the radiation.

Table 4

Working characteristics of different types of incandescent lamps

	voltage dependence of		
	vacuum-lamp	gas filled lamp	halogen-lamp
Current	$I \sim U^{0,6}$	$I \sim U^{0,5}$	$I \sim U^{0,6}$
Power	$N \sim U^{1,6}$	$N \sim U^{1,5}$	$N \sim U^{1,6}$
Light flux	$\sim U^{3,6}$	$\sim U^{3,8}$	$\sim U^{3,0}$
Efficiency	$\sim U^{2,0}$	$\sim U^{2,3}$	$\sim U^{1,4}$
Life expectancy	$L \sim U^{-14}$	$L \sim U^{-14}$	$L \sim U^{-14}$

Especially for high current types of lamps the current is regarded as primary variable. It is, however, always necessary to measure at the same time the lamp voltage as well, as only this can supply the user with some information as regards the condition of the lamp, one might be nearly certain that the lamp emits the original

spectral distribution only if for rated current the resistance stays unchanged. A typical measuring set-up is seen in Fig.7. According to older practice storage batteries and variable resistors have been used as current source. The use of current stabilizers simplifies the current setting problems considerably, as no high current regulators, heat producing resistors, etc. are needed. The problem of measuring the spectral power distribution of standard lamps will be discussed in more detail in Sec.7.

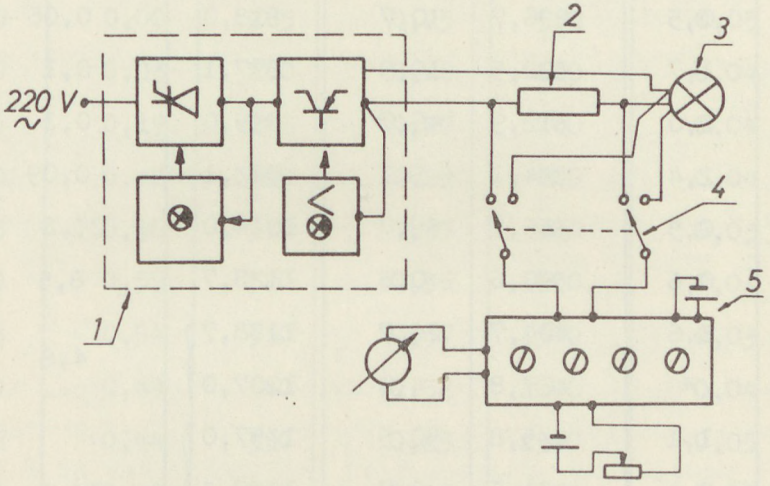

Fig. 7

Measuring set-up of incandescent lamps

1 - Current stabilizer; 2 - Precision resistor; 3 - Lamp under test; 4 - Current-voltage measuring switch; 5 - Potentiometer

Incandescent lamps, even if colour temperatures higher than 3000 K are used, are poor emitters in the ultraviolet. It has become common practice to use the UV-Standard of Krefft, Rössler and Rüttenauer for standardizing UV-fluxes. This is a special mercury vapour lamp,

Table 5a.

Spectral irradiance of the UV-Standard

Irradiation in 1 m distance for the lines

λ [nm]	E [µW/cm²]	λ [nm]	E [µW/cm²]	λ [nm]	E [µW/cm²]
230,2	1,1	292,5	1,1	772,9	0,08
232,3	0,5	296,7	10,7	818,0	0,06
235,2	1,7	302,5	19,9	877,1	0,1
237,8	2,0	312,9	46,7	899,0	0,1
240,0	2,4	334,1	5,1	943,1	0,09
244,6	0,5	365,7	69,7	1014,0	23,8
246,4	0,6	390,6	0,6	1128,7	8,5
248,3	6,6	404,7	26,7	1188,7	4,8
253,7	*	407,8	4,0	1207,0	
257,6	1,1	435,8	50,5	1357,0	
260,3	0,4	491,6	0,7	1367,3	14,0
264,0	0,4	546,1	62,8	1395,1	
				1530,0	3,24
265,3	16,2	578,1	51,4	1691,8	
269,9	3,1	623,4	0,1	1693,9	10,9
275,7	2,7	671,6	0,08	1710,8	
280,4	7,1	690,7	0,6	1719,3	
289,4	4,1	708,7	0,2		

---

* Line-reversal

Table 5b.

Spectral irradiance of the UV-Standard

Spectral irradiance in 1 m distance for the continuum

λ [nm]	E [$\mu W/cm^2 nm$]	λ [nm]	E [$\mu W/cm^2 nm$]	λ [nm]	E [$\mu W/cm^2 nm$]
200	0,00	280	0,26	550	0,05
205	0,00	285	0,25	580	0,05
210	0,03	290	0,26	600	0,04
215	0,19	295	0,27	700	0,04
220	0,42	300	0,29	800	0,04
225	0,56	310	0,33	900	0,03
230	0,59	320	0,36	1000	0,04
235	0,54	330	0,37	1500	0,03
240	0,49	340	0,32	2000	0,04
245	0,44	350	0,25	2500	0,05
250	0,38	360	0,18	3000	0,07
253,4	15,08	370	0,12	3500	0,08
255	7,77	380	0,09	4000	0,15
260	1,67	390	0,07	4500	0,21
265	0,85	400	0,07	5000	0,18
270	0,43	450	0,05	5500	0,14
275	0,30	500	0,04	6000	0,11

with a vapour pressure of appr. 1.5 at.[10] The spectral irradiance data seen in Table 5a and b. are only approximative, their absolute value changes somewhat from lamp to lamp. The relative spectral distribution of these lamps is, however, very stable /<0.5%/ and independent of the individual properties of the lamps. The lamps are produced /e.g. Osram, Philips/ in 250 W size and have to be fed with a constant d.c. current of 2.00 A. The lamp has to be used in a vertical position in an enclosure not smaller than 2000 cm^3.

4.2 Excitation sources

For the excitation of luminescence and the irradiation of chemical, or biological samples it was usual to use some sort of discharge tube. In the following the most important characteristics of such sources, as well as of some lasers whose importance as excitation sources is rapidly growing, will be summarized.

4.2.1 Mercury discharge-lamps[11]

Mercury discharge-lamps, as also all other types of discharge-tubes are lamps with negative characteristics and thus can be operated with ballast chokes or resistors. It is usual to group the Hg-lamps according to the pressure of Hg filling under operating conditions.

Low pressure mercury burners have usually working vapour pressures of approximately 0.005 - 0.1 torr. Under such conditions the emission in the UV-C range /at 254 nm/ is prevailing, in many applications the radiation emitted in the other Hg-lines can be neglected. Table 6 shows typical spectral distribution for such a lamp /NM 15/40/. Regarding the measurement technical application of such lamps it has to be mentioned that the intensity of radiation in the 254 nm Hg-line, and the relative intensity of the single lines is highly pressure, and thus

Table 6

Intensity distribution of some mercury lamps

	Q 300	ST 42	ST 75	NM 15/40
Working vapour pressure approx.atm	1	0.5	5	0.006
Relative intensity of the lines 238[nm]	3	2	2	
240	3	2	2	
248	20	11	7	0.1
254	81	150	30	100
265	26	33	17	0.9
270	4	3	2	0.1
280	9	9	6	0.1
289	6	7	5.5	0.1
297	16	20	15	0.6
302	32	28	25	0.4
313	71	81	55	2.8
334	7	7	7	0.1
365	200	200	200	2.2
405-7	32	59	43	1.6
436	69	84	67	1.1
546	68	203	95	1.6
577-9	65	54	70	0.5
Radiant flux UV-A W	6.5	0.7	3.4	
UV-B W	7.0	0.7	3.6	
UV-C W	5.5	0.6	3.8	6.0

temperature dependent. Even a small change in wall-temperature due to unwanted air movements in the laboratory can change the radiant flux. In many cases the normal lamps produced for sterilization and bactericidal applications can be used. /These are usually available in two types: producing Ozone and those avoiding the generation of Ozone/.

For special measurement technical applications lamps with higher radiation density are also available, containing a discharge section of capillary design. Table 7 contains some basic information on the elctrical characteristics of Hg-lamps.

Table 7

Electrical parameters of mercury lamps

	Q 300	ST 42	ST 75	NM 15/40
Burner voltage [V]	110	41	90	58
Burner current [A]	2.6	0.65-1.2	0.95	0.35
Burner loading [W]	240	23-36	80	15

Attention has to be drawn to the fact that the radiation of low pressure Hg-lamps is extremely hazardous on the eyes, thus the use of eye protective goggles is always necessary if the eyes are exposed to direct or scattered radiation of such lamps.

High pressure mercury lamps are less affected by the temperature of the surrounding air: nevertheless too low or too high ventillation of the lamp-housing is to be avoided as both the raising and falling of the working temperature above or below the nominal value is

dangerous for the lamp: it might extinguish or even explode, the life ratings become in every case impaired.

In optical laboratories it is common practice to use the burner of general use high pressure Hg-lamps as UV-exitation units. For such burners it is even more important to keep them a proper enclosures as these lamps are not protected against the influence of the environment.

Peculiarity of these lamps is that the arc usually moves in the discharge tube. Although this has no effect on the total emitted radiation, in optical investigations when the arc is focussed onto some sample or optical element, this can seriously influence the measurement. Special lamps have been constructed /e.g. by Quarzlampen Gesellschaft m.b.H, Hanau the so-called St types/ that overcome this failure, but only on the expenses of some loss in radiant efficiency.

The radiation of high pressure Hg-lamps can be further improved if a d.c. current stabilizer is used as power supply.

Relative and absolute intensity values of some typical high-pressure lamps are seen in Table 6, their basic electrical data being disclosed in Table 7. It has to be mentioned that for these lamps, similar to the UV-standard lamp, the gap between the lines is already partly filled up with a continuum /see Table 5/.As seen from Table 6 these lamps emit the biggest part of their radiation in the lines grouped around 366 nm. Nevertheless it has to be kept in mind that values as indicated in Table 6 are only approximate, the relative and absolute spectral power distribution might change from one sample of a lamp type to the other, or even it changes with ageing and environmental influences.

The extra-high pressure /EHP/ Hg-lamps emit a considerable amount of their energy in the continuum, the lines become broadened up. The spectral power distribution extends from the middle of the short wavelength ultraviolet till the end of the visible spectrum /see Fig.8/.

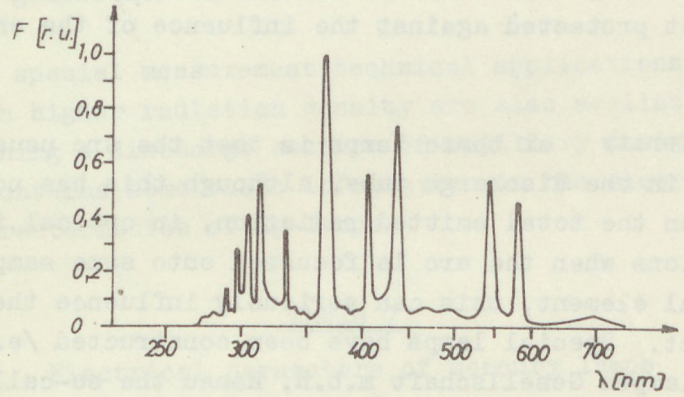

Fig. 8

Relative spectral power distribution of an HBO 500 type Hg-lamp

The arc is highly concentrated in these lamps, their radiant emittance is extremely high. However, the problem having already been encountered when dealing with the high pressure lamps, becomes here more severe: the location of the arc is instable, it moves especially in less well constructed types and lamps at the end of their life rather strongly. Usually d.c. types show more stable lighting.

The EHP Hg-lamps need a special ignition. This is performed by producing a high voltage /several kV/ pulse on either a special ignition electrode or directly into the main current lead. Fig. 9 shows the block diagram of the lamp circuitry using an ignition transformer.

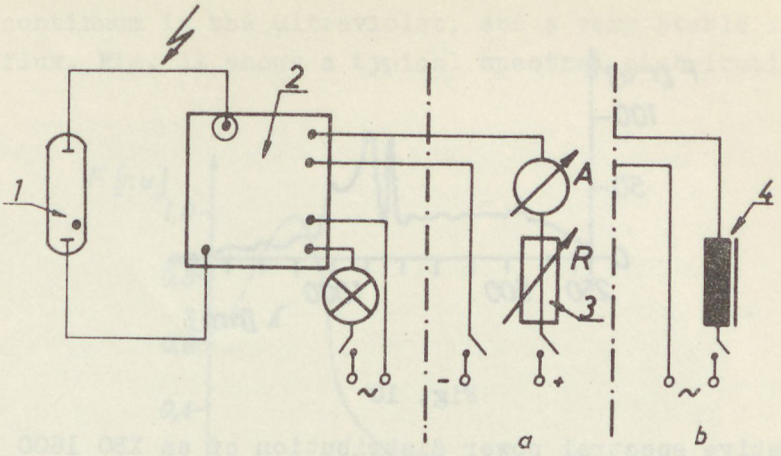

Fig. 9

Bock diagram of the lamp circuitry of an EHP Hg-lamp
a - d.c. supply; b - a.c. supply

It has still to be mentioned that these lamps emit a rather strong ultraviolet radiation hazardous both for the eyes and skin. Furtheron as the inner pressure is, during operation, considerable, an explosion hazard cannot be avoided. Thus it is necessary to operate these lamps in well dimensioned and ventillated enclosures, and it is not permitted to open these before the lamp has cooled down. Eye protective goggles are to be used.

4.2.2 Xe-lamps

The high pressure Xe-lamps can be used with great advantage in different spectrometric and colorimetric applications. They generate a large amount of energy throughout the ultraviolet, visible and infrared region of the spectrum. Fig. 10 shows the relative spectral emission of an XBO 1600 lamp, the spectral distribution of other types is rather similar.

The main drawback of the Xe-lamps is the arc movement, which is even worse than in EHP Hg-lamps.

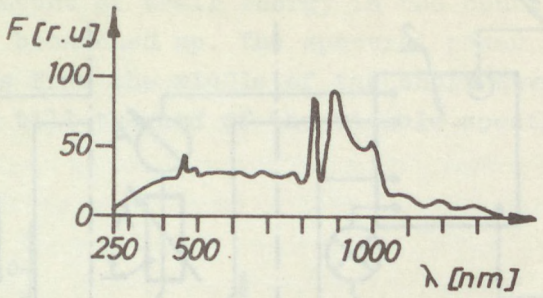

Fig. 10

Relative spectral power distribution of an XBO 1600 Type Xe-lamp

Regarding the starting characteristics and hazard of Xe-lamps, they are rather similar to the EHP Hg-lamps, only the interior of Xe-lamps stays, also if cold, under high pressure, therefore it is always necessary to store the lamps in protective enclosures. The mounting and dismounting of lamps has to be performed with utmost care, using eye protective goggels and shields, as well as strong gloves.

We mention it here, but it is valid for all similar lamps that burners caped on both ends must not be rigidly mounted on both ends, one of the current lead has to be kept flexible. The ballon of every lamp, manufactured of quarz glass is highly sensitive to oil or grease contaminations. The bulb must not be touched by hand /gloves should be worn when handling them and they should be cleaned with alcohole or CCl_4 before usage/.

4.2.3 Deuterium lamps [12]

If a continuous ultraviolet radiation is required, and the radiant flux has not to be too high, deuterium lamps can be used advantageously. They have a broad

continuum in the ultraviolet, and a very stable radiant flux. Fig. 11 shows a typical spectral distribution.

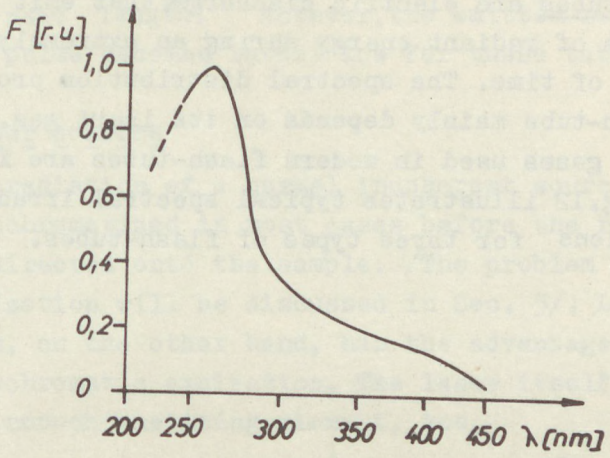

Fig. 11

Relative spectral power distribution of a deuterium-lamp

The 0.3 A, 100 V types of these lamps are often used in ultraviolet spectrophotometers as radiation sources, for special purposes H_2-, or D_2-lamps of several hundreds of watts consumption are also available. They usually require d.c. voltage, with an appropriate serial resistance.

4.2.4 Miscellaneous excitation sources

For special purposes carbon arc lamps have been used. They emit a strong radiation both in the ultraviolet and visible. Due to the special care that is required in manipulating with the free burning coal electrodes, the carbon arc lamp becomes less popular.

The speciality of the Zirconium concentrated arc lamps is the very small /ϕ = 0.1 mm/ size of the luminous

spot. They emit a continuous radiation peaking in the infrared, with some superposed spectral lines.

Flash-tubes are electric discharges that emit large amounts of radiant energy during an extremely short period of time. The spectral distribution provided by a flash-tube mainly depends on its inert gas. The most common gases used in modern flash-tubes are Xe, Ar and Kr. Fig.12 illustrates typical spectral irradiance distributions for three types of flash-tubes.

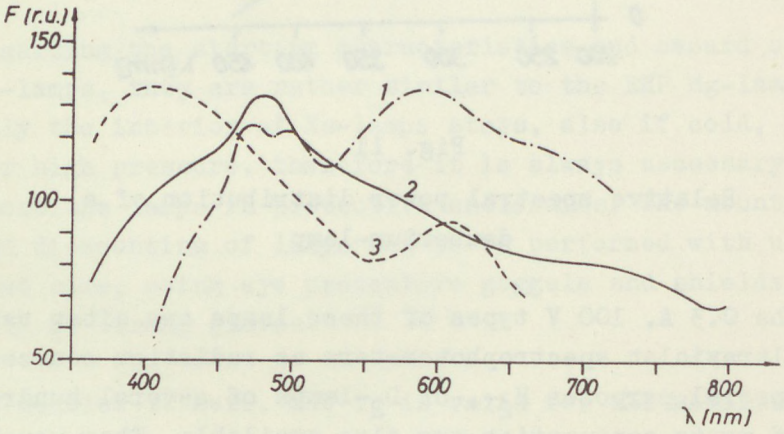

Fig. 12

Relative spectral power distribution of three types of flashtubes [13]
Curve 1: xenon; curve 2: 90 % krypton and 10 % xenon; curve 3: argon

Flash-tubes are often used in kinetic investigations, for instance luminescence afterglow measurements. For such purposes it is very important that the subsequent flashes should have the same light sum /emit the same amount of radiant energy/ and besides the spectral distributions the time-distribution of the flashes becomes

important. Usual flash-tube and strobing equipments enable a pulse-length of 1-100 μsec. For shorter pulses special lamp- and excitation apparatus constructions are necessary. The best flash-tubes produce light pulses of nsec length, however, the emitted radiant energy per pulse becomes rather low for these tubes.

4.2.5 Laser sources

The radiation of a normal incoherent source has to be monochromatized in most cases before the radiation can be directed onto the sample. /The problem of monochromatization will be discussed in Sec. 5/. Laser excitation, on the other hand, has the advantage of direct monochromatic excitation. The laser itself might contain the monochromatizing element, too.

A detailed discussion of this modern and rapidly growing field of radiation sources is far beyond the possibilities of the present paper. Our aim is only to draw the attention to these important sources, as it can be taken for granted that the importance of laser sources will grow also in the field of luminescence, photochemistry and biology.

From the point of view of application we might devide the lasers into two main classes: continuous operating ones and pulse operated lasers. Main representatives of the first class are the gas-lasers. Almost every gas laser can be operated continuously, its well-focussed, highly monochromatic radiation can easily be focussed on the sample. If synchronous detection is used /see Sec. 6/, a light chopper might be applied. The laser, if properly adjusted, is less noisy than a conventional source of equal bandwidth, a further advantage in some experiments. A question, attention has to be paid to, is that laser radiation is highly polarized. If crystals or materials with definite structure or optical activity

are investigated, this has to be kept in mind. For irradiation purposes multimode laser operation, yielding a higher outpot power, is usually adequate.

Pulse lasers with well-defined lasing characteristics are the optically exited solid state lasers and some gas lasers /e.g. N_2/. The dye-lasers have the advantage of being tunable in a given wavelength range, but their output is less monochromatic /they posess in some cases a bandwidth of several Angströms/.

A growing branch of the laser family is the electroluminescence or injection laser. All the other laser sources are still bulky, either high voltages or some form of flash tube or other optical, in some cases electron current, excitation is necessary to make them work. Injection lasers, on the other hand, are tiny solid state devices, they work without external resonators, only low or medium power electronics are needed. Up to

Table 8

Some Laser-Lines Used in Spectrometry

He-Ne laser	632,8 nm
Xe-laser	3,507 µ
	5,5739 µ
A ion-laser	448,0 nm
N_2	3371 nm
Chloro-aluminium-phtalocyanine	755,0-763,0 nm*
Acridone in ethanol	437 nm
Fluorescein in water	527 nm
Rhodaminde 6 G	555 - 610 nm*

---

* Dependent on solvent and concentration

now good efficiency /room temperature, continuous operation/ could be achieved only in infrared emitting diodes, but principally it is possible to find some materials enabling the manufacture of short wavelength injection lasers as well.

At the present stage of lasers it is possible to produce laser radiation at virtually any wavelength starting from the edge of the vacuum ultraviolet, far into the infrared region. It would be even hard to enumerate all the useful laser lines tabulated in literature. Table 8 contains data on some useful laser sources.

5. Monochromatization

Problems related to the monochromatization of the exciting /and in case of luminescence, emitted/ radiation are multifold. Instead of a systematic treatise of filters and monochromators, only some problems and their possible elimination will be discussed.

5.1 Filters

In optical laboratories one encounters mainly three types of filters: glass-filters, interference filters and gelatine filters /liquid- and special types /e.g. Krystiansen/ of filters will be neglected, just as we do not deal here with neutral and polarisation filters/.

The glass filters fall again in two broad categories: short wavelength cutoff filters and bandpass filters. Usually it is possible to filter a source concerned only with more filters placed one behind the other. In doing so one has to pay attention to two facts: Some filters are affected if exposed to strong UV-radiation /the filters solarize/. This produces a small devitrification, changes the trans-

mission characteristics. Especially the filters having a high transmission in the UV-C region tend to solarize, their short wavelength transmission might drop considerably even if the long wavelength transmission stayed unchanged. Thus the most delicate /least stable/ filter has to be placed farthest from the source. The second problem often encountered is that some filters show luminescence under UV, or even short wavelength visible irradiation. Filter catalogues usually give some hints whether a particular filterglass is stable or not, and whether it fluoresces or not, but the spectral distribution of this luminescence /it might lie even in the infrared/ is usually not given. Thus the user has to find some more filters which cut this luminescence as well.

Sometimes the temperature dependence of the transmission characteristics causes some difficulties. Both, the cutoff wavelength of cutoff filters and the wavelength of maximum transmission /and absorption/ of band filters varies with temperature. Fig. 13 gives some examples of such changes.

It may be obvious that filters are delicate glass-ware, prepared sometimes of rather soft or hygroscopic materials. They have to be handled, cleaned and used with utmost care. Before staggering filters one on top of the other, they have to be cleaned, and afterwards sealed with adhesive tape, so that dust should not settle between the glasses, it is good to bring the glasses in thorough contact /without fringes due to residual air/. The residual transmission of such filter packs can be calculated by simply adding the densities, interfilter reflections have to be taken into consideration only if they are used for calibrating purposes.

The family of <u>interference filters</u> branches again into two main sorts: metal interference filters and all dielectric ones. The principle of operation, using an optical reso-

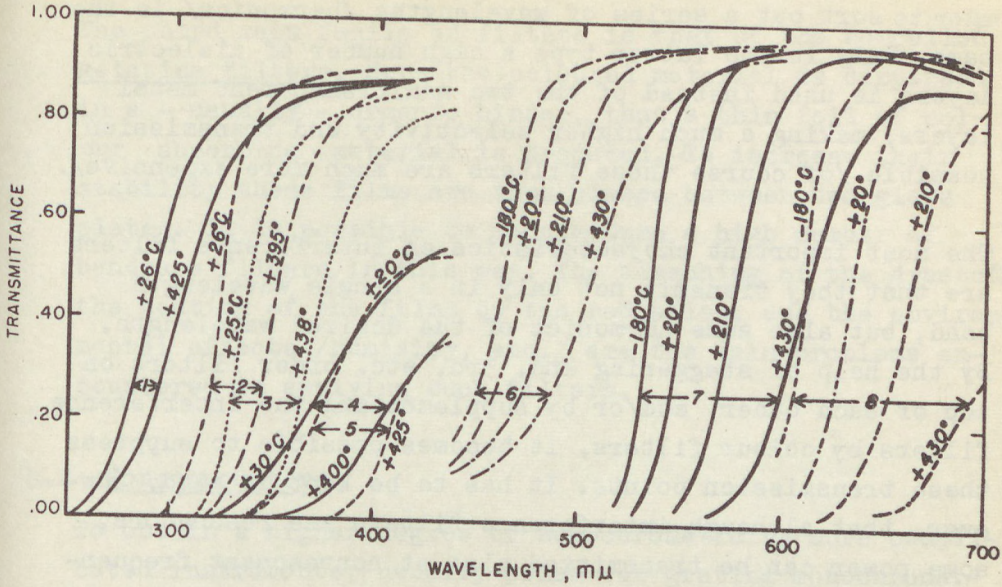

a

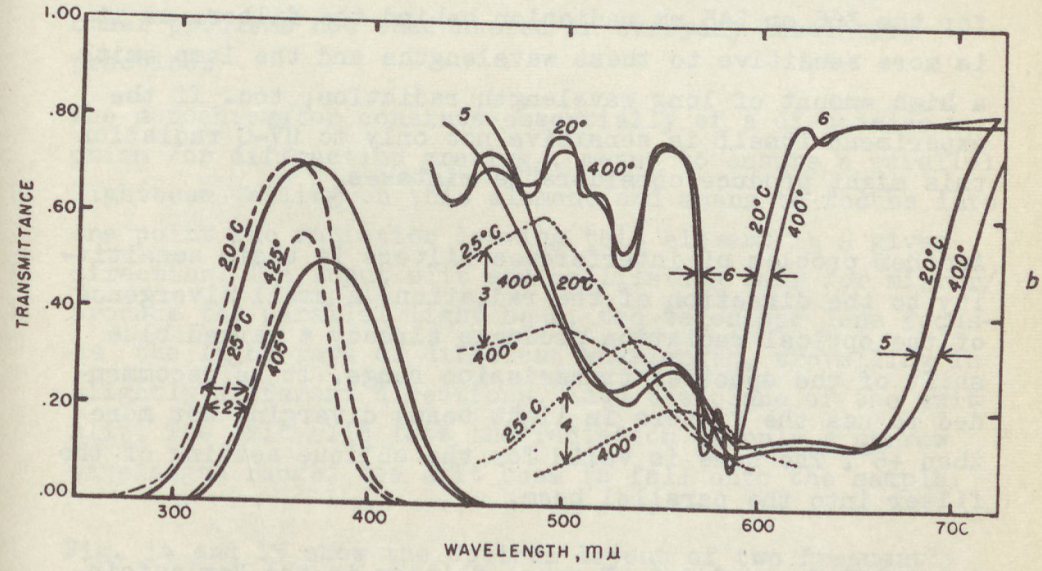

b

Fig. 13

Transmission curve of some cutoff /Fig. 13.a/ and band-filters /Fig. 13.b/ [14]

nator to sort out a series of wavelengths /harmonics/ is the same. Only in the latter type a high number of dielectric layers is used instead of the two semitransparent metal layers, making a much higher selectivity and transmission possible /of course these filters are much more expensive/.

The most important characteristics of interference filters are that they transmit not only in a single wavelength band, but also some harmonics of the desired wavelength. By the help of staggering 2nd, 3rd, etc. order filters on top of each other, and/or by supplementing the interference filters by colour filters, it becomes possible to suppress these transmission points. It has to be kept in mind, however, that although interference filters are resonators, some power can be transmitted also at nonresonant frequencies. Thus it can happen, for instance, that filtering the 254 nm line of a high pressure Hg-lamp by a 254 nm interference filter, the system detects the radiation signals for the 366 or 546 nm radiation behind the filter, as it is more sensitive to these wavelengths and the lamp emits a high amount of long wavelength radiation, too. If the experiment itself is sensitive not only to UV-C radiation this might produce considerable mistakes.

Another problem of interference filters is their sensitivity to the direction of the radiation. A small divergence of the optical radiation produces already a marked blue shift of the spectral transmission range. It is recommended to use the filters in light beams diverging not more than $\pm 5^{\circ}$. The same is valid for the oblique setting of the filter into the parallel beam.

A special form of interference filters is the Verlaufsinterferenzfilter. Here the wavelength of transmission maximum changes in the plane of the filter. Thus if the filter surface is scanned with a small light beam, a monochromatic radiation of variable wavelength can be produced.

The third main family of filters is that of the so-called gelatine filters. Here the coloured material is dispersed in a - usually - organic binder, thus a thin foil of colour absorbing material is produced. To increase their stability these films are then placed between two glass plates. It is possible to manufacture a high number of bandpass filters in this way. The bleaching of the dyestuff, the heating of the films by the radiation, and the environmental effects /humidity, etc./ are the main problems encountered in applying such filters.

5.2 Monochromators

To obtain a higher degree of monochromaticity more complicated instruments, usually prism or grating monochromators, are needed. In the following the most important factors influencing the use of monochromators will be discussed, but we will not deal with construction details or other problems not encountered in everyday laboratory practice.

The monochromator consists essentially of a dispersive prism /or diffraction grating/, means to ensure a parallel lightbeam falling on this element and means to focuss into one point the radiation leaving this element in a given direction. The input slit and collimating lens /or mirror/ produce the parallel light beam, the telescope lens focuses the light rays of different wavelength, travelling in slightly different directions, into the plane of the exit slit. The exit slit lets the radiation of only a narrow wavelength range, the exit beam to fall onto the sample.

Fig. 14 and 15 show the optical layout of two frequently adopted monochromator setups. Both systems have the advantage that the spectral band just used travels always under minimal deviation through the instrument. The Littrow mounting /Fig. 14/ has the further advantage that only half the amount of the prism material is necessary to prod-

uce the same resolution as in the Wadthworth mounting /Fig.15/. On the other hand, the latter has the advantage that the observer does not see the collimating mirror which is illuminated by white light and thus any imperfection on its surface /scratches, dust particles, etc./ scatters light. In Litrow's mounting this scattered light reaches the observer unattenuated.

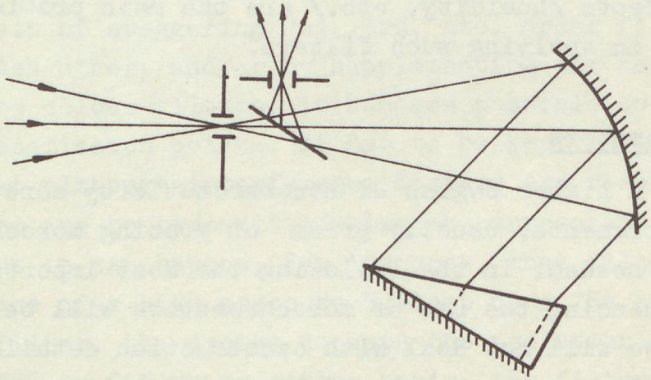

Fig. 14

Optical layout of a Littrow mounting

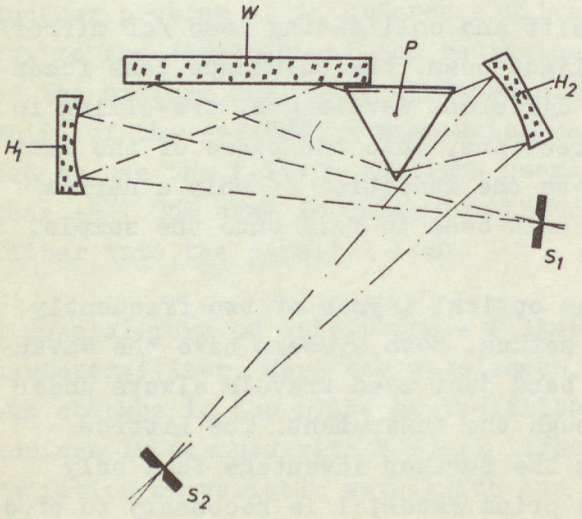

Fig. 15

Optical layout of a Wadthworth mounting

Fig. 16 shows the sketch of a double monochromator. Such systems have the advantage of strongly reducing the scattered radiation. If the two monochromators are mounted in such a manner that both of them disperse light with the

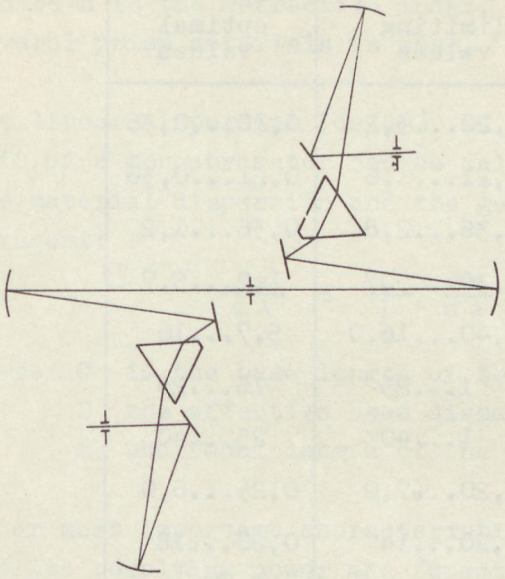

Fig. 16

Optical layout of a double monochromator with additive dispersion

same angle direction, they are called to work with additive dispersion. If the direction of the dispersion is opposite in the two monochromators, one speaks of substractive dispersion: In this case, if the middle slit is opened the radiation in the output slit contains an increasing amount of radiation composed of different wavelengths. By this set-up it is possible to change the spectral distribution of a radiation: instead of the middle slit a template is placed showing different heights at the position of the different wavelengths, letting through different amounts of radiation. The second monochromator recomposes the dispersed spectrum, but by this change in the weight of different wavelengths can be produced. Such an instrument is often called vario-illuminator.

Table 9 contains some information of commonly used prism materials. The usefulness of a dispersive material is de-

Table 9

	Useful wavelength range [μ]	
	limiting values	optimal values
Quarz	0,20...3,2	0,20...0,36
NaCl UV	0,21...1,6	0,21...0,36
Flintglas	0,36...2,8	0,36...1,2
Lithiumfluorid	0,30...5,7	1,2...5,7
NaCl UR	0,40...16,0	5,7...16
Kaliumbromid	1...25	16...25
KRS 5	1...40	25...40
CaF_2	0,20...7,0	0,25...6,0
KCl	0,20...14	0,20...18

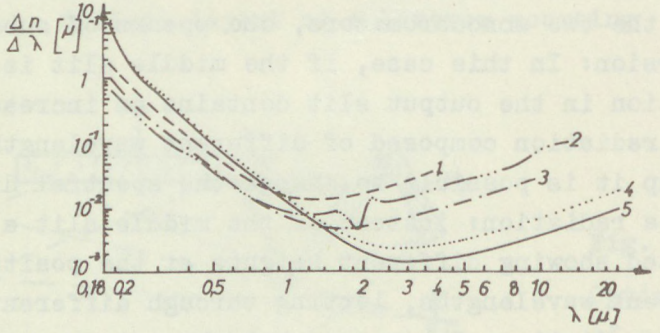

Fig. 17

Material dispersion of several prism materials [15]

termined partly by its transmission and partly by the change of the refractive index, the dispersion, in the wave-

length range under consideration. In Fig. 17 the material dispersion

$$D^x = \frac{d\,n}{d\,\lambda} \qquad 20$$

/where n is the refractive index, λ the wavelength/ of several prism materials is seen.

The linear dispersion $(ds/d\lambda)$ in the plane of the exit-slit of a monochromator can be calculated by the help of the material dispersion and the geometric data of the instrument:

$$\frac{ds}{d\,\lambda} = \frac{C}{D}\,\frac{d\,n}{d\,\lambda}\,f \qquad 21$$

where C is the base length of the prism
D the effective beam diameter
f the focal length of the telescope lens.

Other most important characteristics of a monochromator are its resolving power and /practical/ resolution.

The resolution $(\lambda/d\lambda)$ of a prism monochromator, is given by

$$A = \frac{\lambda\,f}{B\,D}\,C\,\frac{d\,n}{d\,\lambda} \qquad 22$$

where λ is the wavelength, B the slit width, the other symbols are as in Eq. 21. $C\,\frac{dn}{d\lambda}$ is the Raleigh resolving power of the prism. For a grating instrument the resolving power is

$$\frac{\lambda}{d\,\lambda} = m\,N \qquad 23$$

where m is the number of lines taking part in the interference and N the order of the diffraction. This sets a lower limit to the bandpass of the monochromator /wavelength band of the equienergetic spectrum that is transmitted with an attenuation not less than 50 % with respect to the least attenuated part of the spectrum/.

Eqs. 22 and 23 are valid only for infinitezimal slitwidth. In practice, just in case of excitation and irradiation work the slits have to be opened considerably due to energetic reasons. In such cases the wavelength transmission profile is not influenced by the diffraction limited transmission profile, but can be well approximated by a triangle or tetraaeder bound by straight lines:

If monochromatic radiation (λ_0) reaches the entrance slit of a monochromator /e.g. a single spectral line/, and the monochromator is set for this particular wavelength, then the focussed image of the input slit will be observed in the output slit. Changing the wavelength setting of the instrument the "spectral line" /the λ_0 wavelength picture of the input slit/ moves out of the field of vision. It is obvious that if the width of the output slit is equal to that of the input slit, maximal intensity is observed for the wavelength setting λ_0, and the output intensity falls monotonously into both directions moving away from λ_0. If one of the slits is wider and the other narrower, the observed intensity changes as follows: When the narrower slit moves in the image of the wider one, the output intensity stays constant and afterwards falls linearly to zero. Thus, for energetic reasons it is always recommended to use equal input and output slitwidth to obtain highest resolution /smallest bandwidth/. It is usual to define as bandwidth ($\Delta\lambda$) the wavelength range between the two points in the plane of the output slit where the output intensity drops to its half value. Fig. 18 shows this for a well-adjusted monochromator and for one where the input and output slits are set unequally /it is always possible to transform the geometric slit width values by the help of the dispersion into equivalent wavelength range values/.

Spectral bandwidth data attainable in the ultraviolet and visible spectrum with equal input and output slits of 0,1 mm on a Zeiss SPM 1 monochromator /an instrument of

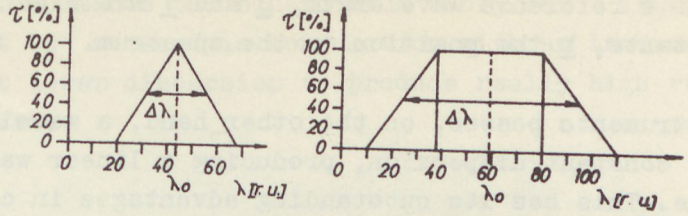

Fig. 18

Transmission curve of an idealized monochromator for equal and unequal slit width settings

middle cathegory: light power 1:6,7, prism heights appr. 45 mm/ are reproduced in Fig. 19. The change in band-width is due to the changing dispersion. This is one of the

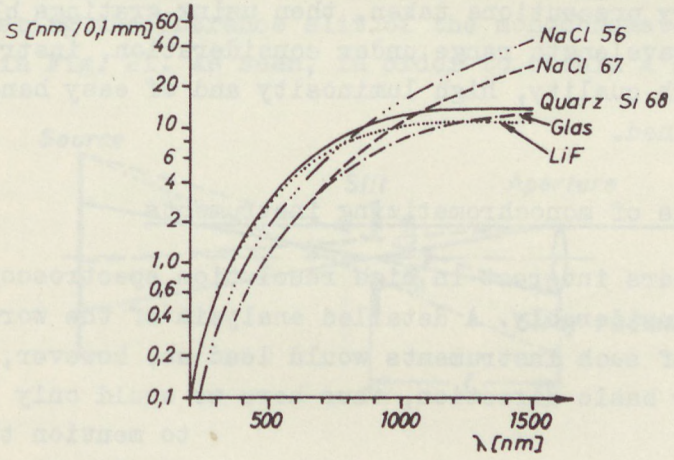

Fig. 19

Spectral band-width curves of a Zeiss SPM 1 monochromator [15]

major disadvantage of prism instruments: The dispersion of a prism changes according to Hartmanns formula:

$$\lambda = \lambda_a + \frac{U}{V-b} \qquad 24$$

where λ_a is a reference wavelength, U and V are experimental constants, b the position in the spectrum.

Grating instruments posses, on the other hand, a wavelength independent constant dispersion, producing a linear wavelength scale. This has its outstanding advantages in calibrating the wavelength scale of the instrument, gives constant bandwidth with a single setting of the slitwidths, and makes the construction of double monochromators easier. The main drawback of grating instruments is that gratings produce a high number of diffracted spectra, and the second, third, etc. spectra can partially overlap: one has to use order-filters, filtering out the unwanted spectra of higher order, which would otherwise coincide with another wavelength of the lower order spectrum in the output slit. If, however, these difficulties are kept in mind, and the necessary precautions taken, then using gratings blazed for the wavelength range under consideration, instruments of high quality, high luminosity and of easy handling can be obtained.

5.3 Other types of monochromatizing instruments

In recent years interest in high resolution spectroscopy has grown considerably. A detailed analysis of the working principles of such instruments would lead us, however, too far from our basic direction, thus here we would only like to mention the growing importance of echelette gratings, of the Lummer-Gehrke plate and different types of interferometers /Michelson and Fabry-Perot/.

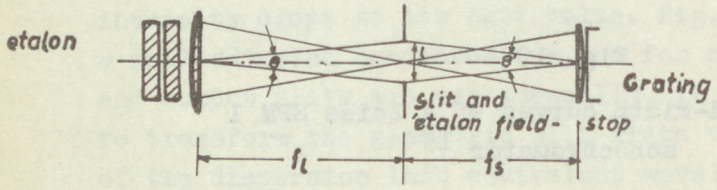

Fig. 20
The combination of a Fabry-Perot and a plane grating spectrometer

Fig. 20 shows the scheme of a Fabry Perot interferometer that can be used in conjunction with an instrument of somewhat lower dispersion to produce really high resolution spectra.

5.4 The input optics of a spectral apparatus [12]

In performing a spectral power distribution measurement or exciting the sample with radiation of a particular wavelength the problem of stray radiation can cause many troubles. It is difficult to estimate and take into correction the effect of stray radiation. Therefore utmost care should be taken to eliminate stray radiation as far as possible.

If a large area source is used, the simplest way of illuminating the entrance slit of the monochromator is depicted in Fig. 21. As seen, in order to obtain a homogeneous

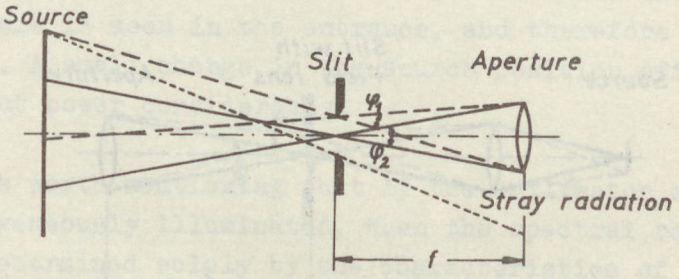

Fig. 21
Input without optics for a spectrometer

illumination of the aperture of the collimating lens /or mirror/, the source has to be moved so close to the entrance slit, that some rays miss the collimator and produce a stray radiation around it.
Similar problems arise if the source is focussed onto the entrance slit of the monochromator by a condenser lens /see

Fig. 22/. To be able to illuminate fully the collimator aperture a high power condensor is needed. If, however, a

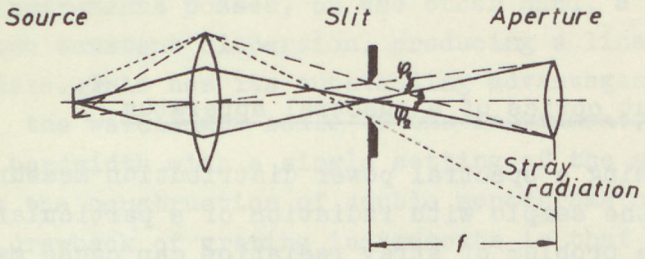

Fig. 22
Simple input optics for a spectrometer

field-lens, as seen in Fig. 23 is placed into the entrance slit, a homogeneous illumination of the collimator aperture can be asured and the same time the aperture ratio of the condenser can be chosen to a smaller value.

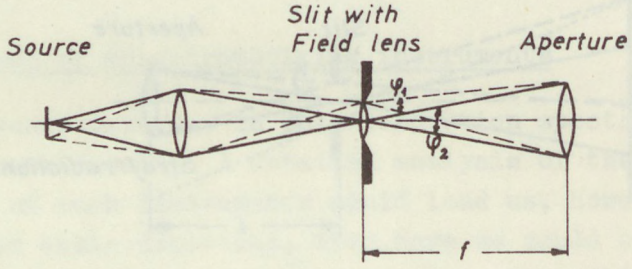

Fig. 23
Input optics with condenser and field-lens

The amount of stray radiation and the necessary area of the source can be reduced by applying a single field lens, as seen in Fig. 24. However, these systems and also those without any optics show the drawback that inhomogenuities of the source are focussed onto different parts of the collimator lens, thus the radiation starting from different

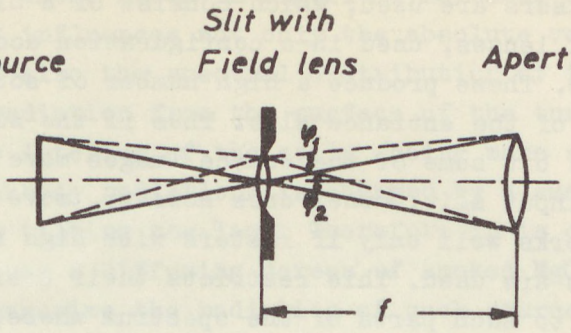

Fig. 24
Input optics using only field-lens

parts of the source travel along different pathes through the optical system. These might have different absorptions, so that the amount of output power will depend on the position of the source. At the same time also the systems where the source is focussed onto the entrance slit of the monochromator suffer from similar drawback: the source picture is seen in the entrance, and therefore in the exit slit. A small change in the source position affects the output power considerably.

It is worth mentioning that if the collimator aperture is homogeneously illuminated, then the spectral radiant flux is determined solely by the characteristics of the monochromator and the radiance of the source, independently of the type of input optics used:

$$P = L\, bh \frac{O}{f^2} \Omega_o \qquad 25$$

where L is the radiance of the source, b the width, h the heights of the entrance slit, O the effective area of the collimator and f the focus length of the collimator.

The arc movement of high and extrahigh pressure lamps has a similar effect, to overcome these difficulties so-called

raster-condensers are used, which consist of a high number of very small lenses, used in a configuration according to Fig. 22 or 23. These produce a high number of source images in the plane of the entrance slit. Thus if the source moves a little bit some of the source images move out of the area of the input slit, other ones however, move into it. The system works well only if rasters with high numbers of single lenses are used. This restricts their useful wavelength range to such parts of the spectrum where, for instance, optics made of plastic can be used.

Another solution is to use a double focussing system, as seen in Fig. 25: the first objective focusses the source

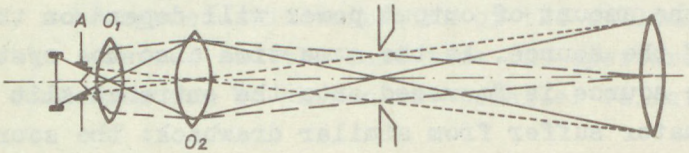

Fig. 25
Input optics using double focusing.
The field-stop A is focused into the collimator lens

into the plane of a second one which, on the other hand focusses the surface of the first one onto the entrance slit of the monochromator. Fieldstop A is focussed by the system of the two objectives into the plane of the collimator, so that the stray light reduction is obtained also with this system. A small movement of the source does not change the illumination of O, considerably thus the radiant flux strays constant as well.

At this point we would like to come back to the problem of focussing the light of a coiled filament spectral distribution standard into the monochromator: If an arrangement

according to those shown in Fig.21-24 is used, a slight displacement influences not only the absolute value of radiation, but also the spectral distribution of it: The proportion of radiation from the surface of the tungsten wire and from the interior of the coils /being more similar to that of blackbody radiation/ is changed by a small displacement or by tilting the lamp. Therefore it is common practice to use a diffusing screen of smoked MgO or pressed $BaSO_4$ to homogenize the radiation of such sources. Naturally, the reflectance characteristics of this diffusing screen have to be taken into consideration when a spectral energy distribution calibration is made. The absolute spectral reflectance curve of smoked MgO is seen in Fig. 26.

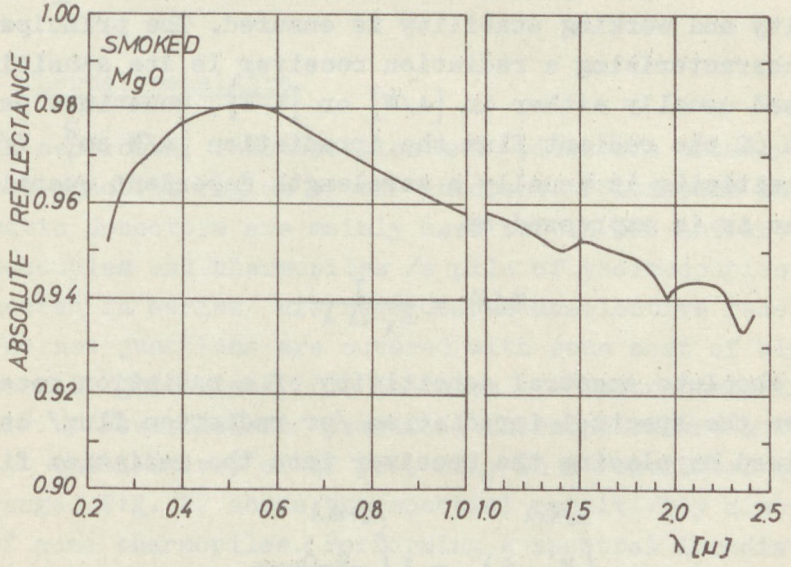

Fig. 26
Absolute spectral reflectance of smoked MgO [16,17]

6. Radiation receivers

The three, for measurement purposes most important classes of radiation receivers are the thermal receivers /for the visible and ultraviolet range of the spectrum mainly thermophiles/, the photoemissive receivers /mainly photoelectric multipliers/ and p-n junction detectors /photoelements and photodiodes/. Photoresistors useful in the ultraviolet and visible spectrum, although of great practical importance, have not been developed to a perfection to be useful for spectroradiometric work. Mainly nonlinearities and fatigue effects restrict their use to on-off and simple proportional control and regulation purposes.

In the following only receivers will be discussed, where the linearity and working stability is ensured. The principal data, characterizing a radiation receiver is its sensitivity, expressed usually either in [A/W] or [V/W], sometimes using instead of the radiant flux the irradiation [A/W cm^2; V/Wcm^2]. The sensitivity is usually a wavelength dependent quantity, and then it is expressed as

$$S(\lambda) = \frac{I}{E_\lambda \, \Delta\lambda} \qquad 27$$

If the absolute spectral sensitivity of a radiation receiver is known the spectral irradiation /or radiation flux/ can be determined by placing the receiver into the radiation field.

$$\int_{\lambda_o-\Delta\lambda}^{\lambda_o+\Delta\lambda} E_\lambda \, d\lambda = I \int_{\lambda_o-\Delta\lambda}^{\lambda_o+\Delta\lambda} \frac{d\lambda}{S(\lambda)\Delta\lambda} \qquad 28$$

where $\Delta\lambda$ is the bandwidth of the incoming radiation, λ_o the central wavelength.

If no focusing element is used the irradiation in the plane of the receiver is

$$E = \frac{L A_1}{r^2} \Omega_o \qquad 29$$

where L is the radiance of the source, A_1 its area, and r the distance between receiver and source. If, however, a focusing lens or mirror is used in conjunction with the receiver, the irradiation on the receiver is

$$E = \frac{L A_f}{r'^2} \Omega_o \qquad 30$$

where A_f is the area of the focusing element /mirror or lens/ and r' the distance between the focusing element and the receiver; this means that the focusing element - disregarding the absorption and reflexion losses - acts as a source of radiance L.

6.1 Thermal receivers

As mentioned, thermocouples and -piles are usually used in the spectral region of our interest. Bolometers and pneumatic detectors are mainly used but in the infrared. Thermocouples and thermopiles /a pile of thermocouples connected in series/ are regarded as unselective receivers. The hot junctions are covered with some sort of black material /gold black, for instance/ to ensure this inselectivity. Nevertheless, practical thermopiles are not absolutely unselective, or if yes, only in a restricted wavelength range. Fig. 27 shows the spectral sensitivity distribution of some thermopiles. Performing a spectral irradiation distribution measurement, it has to be kept in mind that the measurement-accuracy is influenced by this type of selectivity of the detector.

A further problem, encountered in the work with termopiles, is that these detectors are usually sensitive in a very broad spectral range, influenced by the coating of the junctions and the window material of the thermopile, and

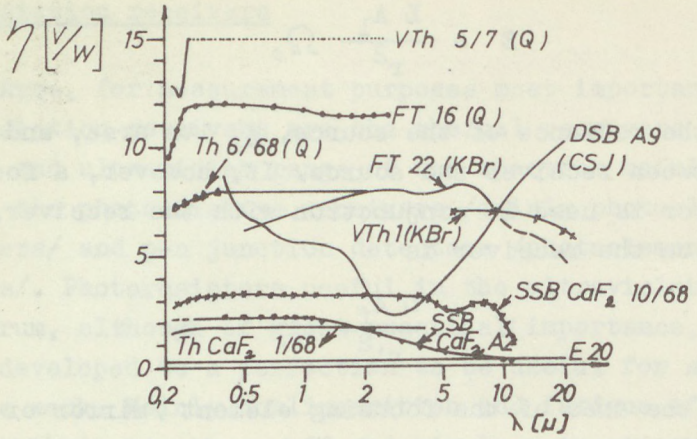

Fig. 27

Spectral sensitivity distribution of several thermopiles [18]

therefore they are extremely sensitive to stray radiation, and also to conducted heat. This problem can be circumvent by using chopped radiation and a.c. measuring techniques. Doing this the radiation has to be chopped as near as possible to the source, and thermopiles with short time constants /and therefore lower sensitivity/ have to be used. In d.c. measurement it is usual to place a shutter in front of the thermopile to be able to set a zero point. If this shutter is not at the temperature of the surroundings, its own radiation can alter the measurement /the losses in an electromagnet actuating the shutter, if close to the light way, can already influence the thermopile readings. If work is restricted to a given wavelength range it is good practice to set in front of the thermopile a filter transmitting only in this range and cutting down all the longer wavelength part of the spectrum.

6.2 Photoelectric multipliers

Present day practice uses in measurement techniques - not regarding the precision photometry - only photoelectric multipliers, giving in the ultraviolet and visible part of the spectrum the highest sensitivity attainable so far.

The spectral sensitivity distribution of multipliers is strongly selective. It is usual to mark the photocathodes, responsible for the spectral sensitivity distribution, by the S-notation or a short form describing tne chemical composition. Fig. 28 shows the spectral distribution of some frequently used photocathodes. It has to be mentioned, however, that knowledge gained from modern semiconductor physics highly promoted the development of modern photocathodes, and thus it became possible to produce highly sensitive cathodes ranging into the infrared spectrum /GaAs cathodes possess threshold sensitivities of 1.5 μ/.

Also the dynode materials have been improved in the last years, and tubes with well-defined single electron maximum

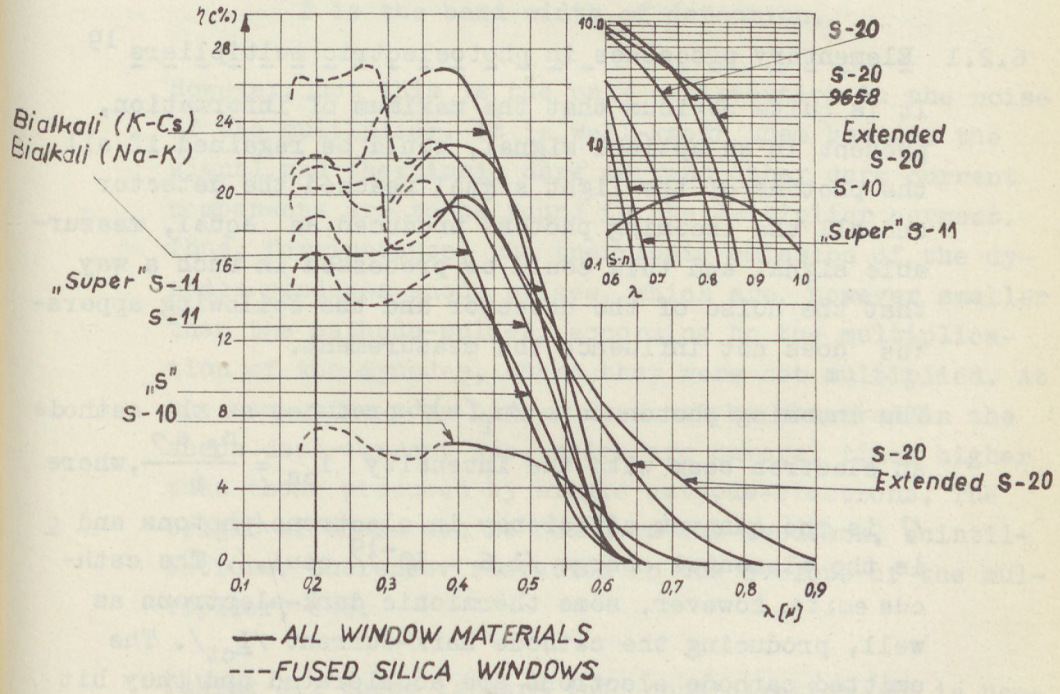

Fig. 28

Spectral sensitivity distribution of several photocathode materials

/a maximum in the pulse height distribution function corresponding to single photoelectrons/ are available /see photoncounting, later in this Section/.

Also the measurement of small photocurrents has become considerably easier in the past years. Several years ago it was common practice to use d.c. techniques with galvanometers or a.c. techniques with light choppers and a.c. amplifiers. Modern operational amplifiers made the amplification of small /10^{-8} - 10^{-10} A/ d.c. currents easy, enabling the construction of detector systems in the laboratory. For a.c. techniques highly sensitive lock-in amplifier systems are available, and for attaining the maximum sensitivity, pulse counting techniques can be used with modern nuclear physical analyzers.

6.2.1 Elementary processes in photoelectric multipliers [19]

It is quite obvious that the maximum of information, present in an optical signal, could be ragained if all the photons of the light signal reached the detector and all the incoming photons produced an equal, measurable signal and this could be processed in such a way that the noise of the detector and the following apparatus does not influence the measurement.

The incoming photon beam /$n_f(t)$/ produces at the cathode an electron beam with the intensity $i_{cs} = \frac{n_f e \eta}{t}$, where η is the quantum-efficiency in electrons/photons and e is the elemental charge /1,6 . 10^{-19} coul./. The cathode emits, however, some thermionic dark-electrons as well, producing the cathode dark-current /i_{ct}/. The emitted cathode electrons are accelerated and they hit with a great probability the first dynode. The probability that the electrons reach the first dynode should be characterised by factor D. The electron multiplication at the dynode is a statistical process with a mean value m.

The secondary electrons ejected from the first dynode will be accelerated again, focused on to the second dynode, and so on, producing a charge pulse at the anode. It can be supposed that the loss of electrons is negligable in the multiplying system itself. The statistical spread in the number of secondary electrons, however, must be taken into consideration. This produces according to Shockley and Pries a factor $B = \frac{m}{m-1}$ in the noise of the anode current. Thus if the anode current were composed only of the signal- and thermionic dark-current, the shot-noise of the anode current would be:

$$\overline{\Delta i} = \left[2e(i_{cs} + i_{ct}) M^2 BD \Delta f \right]^{1/2} \qquad 31$$

where M is the amplification of the whole multiplier and
f is the band-width of detection.

However, not this is the only contribution to the noise of the multiplier. It is well-known that besides the signal and thermionic dark current other dark current components are to be found in the multiplier current. Thus, for instance, the thermionic emission of the dynodes produces anode pulses, which are, however smaller than the cathode-pulses, according to the multiplication of the dynodes, where they were not multiplied. At the same time some high pulses can be observed in the anode dark-current too, which are several times higher than those produced by single cathode-electrons. The origin of these can be found in ion-feedback, scintillations, Cherenkov radiation in the evelope of the multiplier, etc.

Taking all these factors into consideration, it is useful to write the noise current of the multiplier

$$\Delta i = \left[2e(i_{cs} + i_{ct} + \alpha i_{ci}) M^2 BD \Delta f \right]^{1/2} \qquad 32$$

where αi_{ci} stands to show that the high current pulses have an effect as if more electrons had been emitted simultaneously. The signal to noise ratio S/N is given by

$$S/N = \frac{i_{cs}\ D}{\left[2e(i_{cs}+2i_{ct}+2\alpha i_{ci})\ BD\Delta f\right]^{1/2}} \quad 33$$

thus if the quantum efficiency can be made higher, the S/N will be higher too, that is to say, and this is quite obvious, for low level radiometry always a cathode with the highest quantum efficiency has to be chosen. /Optimum values are between 0.1 and 0.3/.

To achieve a higher S/N, the second step is to lower the thermionic cathode current. With modern photocathodes this part of the dark current will already be very low for CO_2 snow temperature.

This means that the noise of a cooled multiplier is composed of the signal noise current and a second noise current component, which might be taken into consideration as a shot-noise current produced by the α times dark-current.

6.2.2 Signal to noise ration in case of different measurement techniques

For measuring the multiplier signal five techniques are usually used:

D.C. measurement
A.C. "
Noise current measurement
Charge integration
Photon-counting

In the first four cases the single noise contributing factors are rather similar. In a.c. measurement half of the information is usually lost due to light-modulation;

d.c. and charge integration techniques are more sensitive to drift problems. The noise current measurement has in this respect its advantages.

The photon-counting brings, however, something quite new. The S/N of $\underline{n}$ counted pulses is given by the statistical spread $\pm\sqrt{\underline{n}}$ of these:

$$S/N = n^{-1/2}$$

If these n pulses are the sum of the n_s signal and n_i dark current pulses, the signal to noise ratio for pulse counting is given by

$$\frac{S}{N} = \frac{n_s}{\left[n_s+2n_i\right]^{1/2}} \qquad 34$$

To compare Eqs. 33 and 34 let us somewhat transform Equ. 33:
Let us first include the probability of cathode-first dynode transition /D/ into the probability of photo- and noise emission. Then one might rewrite the terms for i_{cs}, i_{ct} and i_c:

$$i_{cs} = \frac{n_{cs}e}{t}\ ,\ i_{ct} = \frac{n_t e}{t}\ ,\ i_{ci} = \frac{n_{ci}e}{t} \qquad 35$$

where n_{cs}, n_t and n_{ci} denote the number of cathode pulses in the time interval $\underline{t}$, and

$$n_t + \frac{n_{ci}}{\alpha} = n_i \qquad 36$$

Substituting these quantities into Eq. 33, we receive that for current measurement

$$\left(\frac{S}{N}\right)_{cur.m.} = \frac{\frac{n_{cs}e}{t}}{\left[2e\left(\frac{n_{cs}e}{t}+2\frac{n_t e}{t}+2\frac{\alpha n_{ci}e}{t}\right)B\Delta f\right]^{1/2}} =$$

$$= \frac{n_{cs}}{\left[n_{cs}+2\left(n_t+n_{ci}\alpha\right)\right]^{1/2}\cdot\left(2Bt\Delta f\right)^{1/2}} \qquad 37$$

Comparing Eqs. 34 and 37, taking 36 into consideration it can be seen that if $\Delta f = \frac{1}{2t}$, then the photon counting technique is superior in two respects: 1. factor B does not increase the noise, only the fluctuation of the amplitude distribution of the single pulses; 2. the non-thermal dark current pulses will be evaluated as single pulses and not as the charge carried in them. This makes the pulse-counting technique especially advantageous in low light level measurements.

In the following some practical circuits will be described.

6.2.3 D.C. measuring technique

As mentioned, the use of operational amplifiers enables even in electronics unskilled physicists or chemists to build their simple, inexpensive, but stable, highly linear measuring system. Fig. 29 shows an example for this.

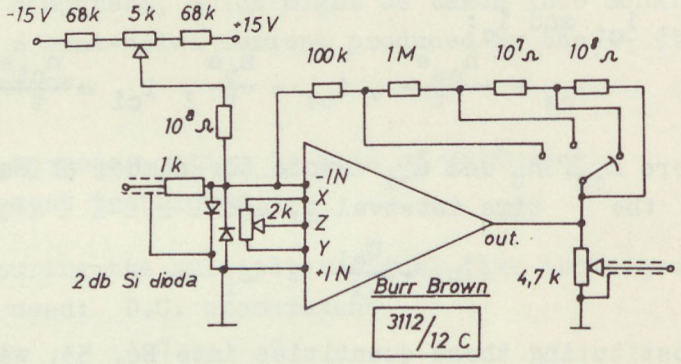

Fig. 29

D.C. amplifier for photoelectric multipliers

P_1 is a potentiometer for counterbalancing the dark current of the multipler, D_1 and D_2 protect the very sensitive input of the amplifier against spontaneous current

surges. P_2 is an inner drift compensating potentiometer. S_1 changes the feedback resistors. Quite generally for 1V output the input sensitivity of such a current amplifying operational amplifier is equal to the reciprocal of the resistivity of the feedback resistor. The time constant $/R_1C_1/$ at the output increases the signal to noise ratio, according to Equ. 33.

This simple system makes high precision work possible, if its output is measured with a precision digital voltmeter and the multipler is fed with well-stabilized high voltage /the stability of this voltage has to be by an order of magnitude higher than the desired stability of the multiplier/.

It is obvious that the amplifier can be built with any operational amplifier supplying a sufficiently high open loop gain, and possessing a low input offset current and current drift /that the offset current flowing into the amplifier should not produce an all too high zero offset at the output/. It is therefore advantageous to use an amplifier with FET-transistor input.

6.2.4 A.C. measuring technique

If it is necessary to decouple the optical information signal from a background, or the darkcurrent of the multiplier varies due to temperature changes, a.c.techniques have to be used. The circuit diagram of a quite simple a.c. amplifier, built with operational amplifiers and possessing a phase-sensitive rectifier to enable us to use the advantages of lock-in techniques, is presented in Fig. 30. The working frequency of this system is 1 kHz, the lowest current that can be measured with this system is 10^{-10} A.

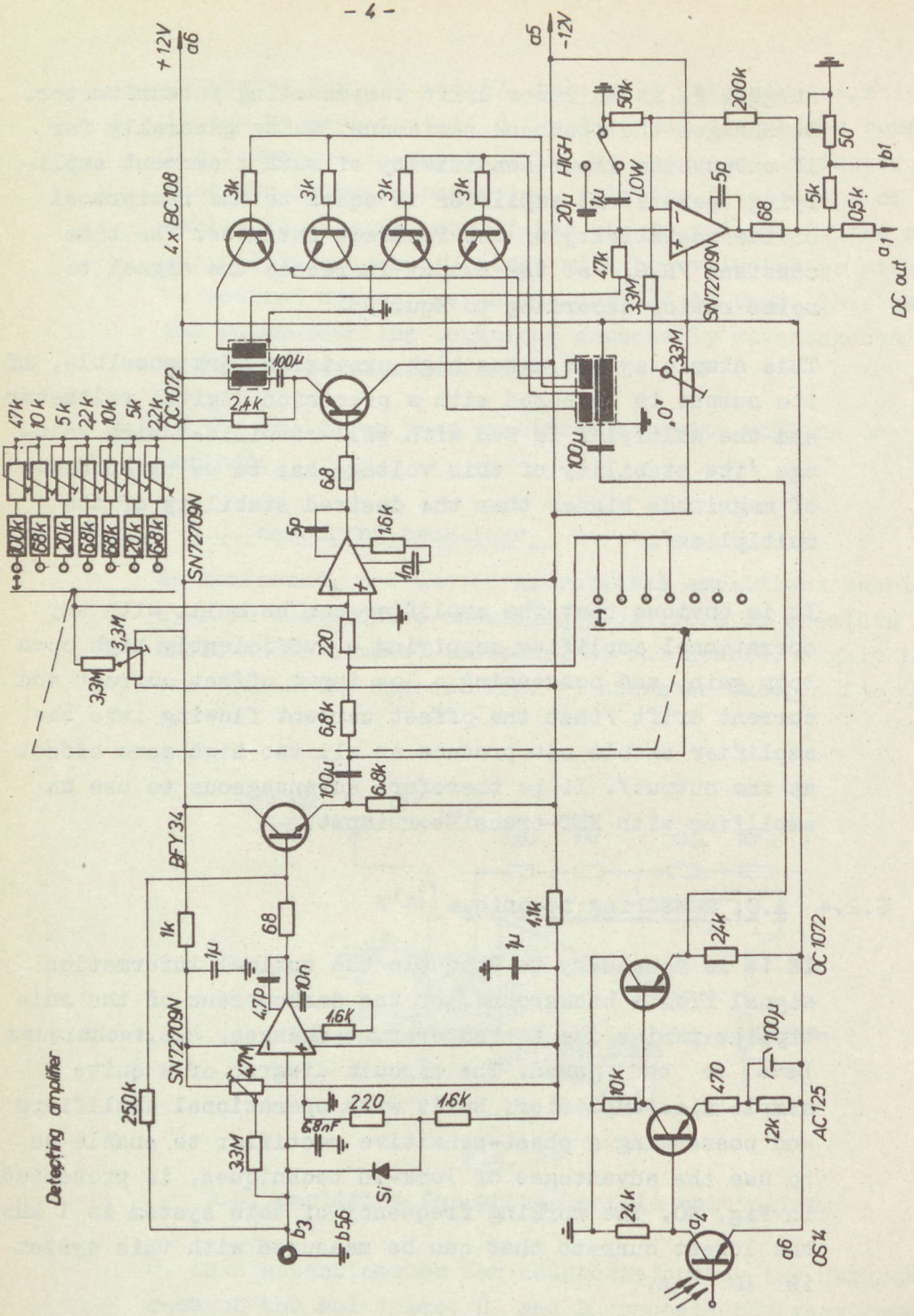

Fig. 30

A.C. amplifier system for photoelectric multiplier [20]

Similar systems can be built from existing apparatuses. Constructing an instrument like this it has to be kept in mind that as the signal intensity is lowered the pulse nature of the single photoelectric events becomes more pronounced. If a multiplier of $M = 10^6$ is used and a current of several times 10^{-10} A is measured with a time constant /in a.c. techniques this placed at the output of the rectifier circuit/ of 5 ~ 10 sec, the noise of this current will be a few times 10^{-12} A, i.e. the measuring accuracy will be lower than 1 %, thus it is not worth increasing further the sensitivity. Even in this case, if the output circuit of the multiplier posesses a stray capacitance of c = 100 pF, the amplitude of the single pulses at the input of the amplifier is in the order of 1 mV $\left(V = \frac{e\,M}{c}\right)$. This lies already on the boarder of overloading the sensitive input circuits of the amplifier. A multiplier of $M = 10^8$ can make serious difficulties if used in this low light level range in a.c. circuitry.

6.2.5 Photon counting techniques

The photon counting technique was introduced in 1941 by Z.Bay, but it has become popular only in the last years, due to the lack of some auxiliary equipments developed in the meantime by the nuclear measuring industry. Nowadays it is usual to have an integrating-differenciating time constant at the anode of the multiplier, producing pulses with a leading edge smaller than 1 μsec and a trailing edge between 1 and 10 μsec. The pulse length determines the highest pulse rate, as pile-up effects have to be avoided. The output pulses of a modern pulse-counting multiplier, in case of a reasonable low-capacitive coupling, are 10 ~ 100 mV high and can be easily amplified by a pulse-amplifier /usually $K \approx 10^3$/. Further processing of the pulses consists of a discrimination against low pulses originating not from single cathode-

electrons /pulses coming from anode near portions of the multiplier, amplifier noise, etc./.

After discrimination the pulses can be counted or, by the help of a rate-meter, transformed into an analogue signal for further processing.

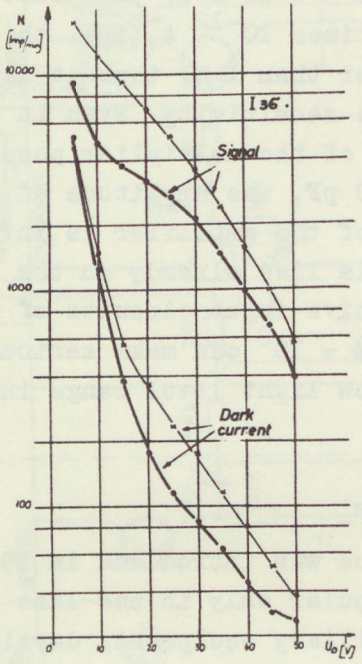

Fig. 31

Discriminator voltage dependence of the dark, and signal pulse-rate /heavy curve: differential discriminator, thin curve: integral discriminator/

The discriminator voltage must be set so that as many as possible of the non-cathode pulses should be eliminated, losing only few signal-pulses /given by the spread due to the factor $\frac{m}{m-1}$/. Fig. 31 shows the discriminator voltage dependence of the pulse rate measured by illuminating the photocathode and in darkness both for the discussed case of a normal discriminator and for a differential discriminator, by the help of which the very high nonthermal dark-pulses can be eliminated. As a matter of fact, it turned out that in case of the multipliers used in our laboratory /unfocused, Venetian-blind ones/ the S/N given by Equ. 34 is for the differential-discriminator in most cases not higher than for the integrating discriminator.

The relative measuring uncertainity $\sigma_r = \sigma/n_s$ has been calculated for a number of signal and dark current pulse

counts.The result of this is shown in Fig.32. Here the σ_r is plotted against n_s. The parameter is the n_i count. Thus, for instance, σ_r = 10 % can be achieved if in the given time-interval 100 signal- and 1 dark-current pulses are observed. But a much lower signal can be observed if the measuring time is made longer. Taking 5000 times longer time, the dark-pulse count will be 5000, and 1000 signal-pulses can still be measured with σ_r = 10 %; that means an intensity which is 500 times lower than that one measured in the first example, and which gives a pulse-rate five times lower than the dark-pulse-rate.

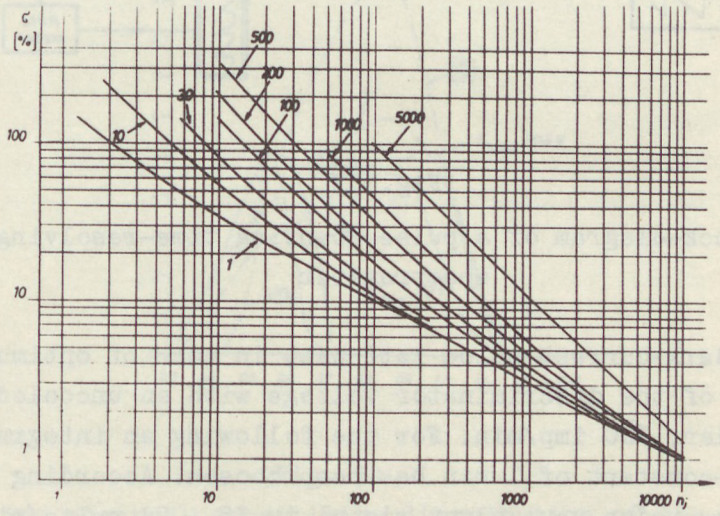

Fig. 32

Relative standard deviation versus signal-count number for different dark current pulse counts

The multiplier, detecting the radiation behind the exit slit, was cooled with CO_2 snow to eliminate the thermionic dark current.

The electronic system consisted of a cathode follower stage, a pulse-amplifier, discriminator and in case of

periodic signals a gate-circuit, the output pulses of which were fed either to a pulse-counting rate-meter, or a scaler. /Fig. 33 shows the block-diagram of the apparatus./

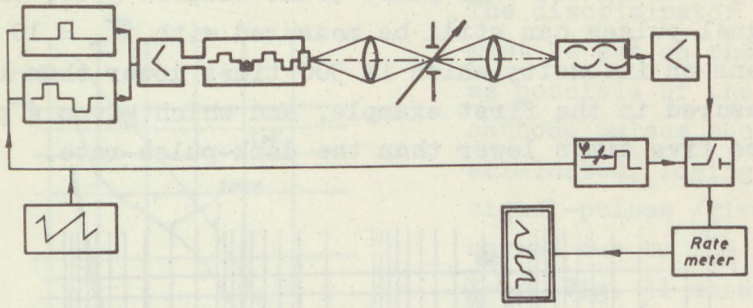

Fig. 33

Block-diagram of a pulse-counting time-resolving spectrometer

The dark-current pulse rate was, in case of optimum setting of the discriminator voltage with an uncooled multiplier, 700 imp/min. For the following an integrating time-constant of 1 min has been chosen. According to Fig. 32 the noise equivalent signal is 38 $\pm$ 24 pulse/min. If this signal should be determined with a higher accuracy ($\pm$ 2σ) the brutto count must be equal to 775 pulse/min. In case of cooling the noise equivalent signal was 30 pulse/min, using the 2σ kriterium. If η = 0.1 is assumed, this means 300 photons/min as the lowest measurable light intensity.

The electronics used allowed to set the highest measured light intensity to 3.10^5 photons/min, thus the dynamics of the apparatus was $1:10^3$.

6.3 Photodiodes and photovoltaic cells

The selenium photovoltaic cell has been for decades the standard receiver in illuminometers. Its most important advantages were:

1. a spectral sensitivity roughly similar to that of the human eye /see Fig. 34/,
2. it produces an electromotive force capable of driving a meter.

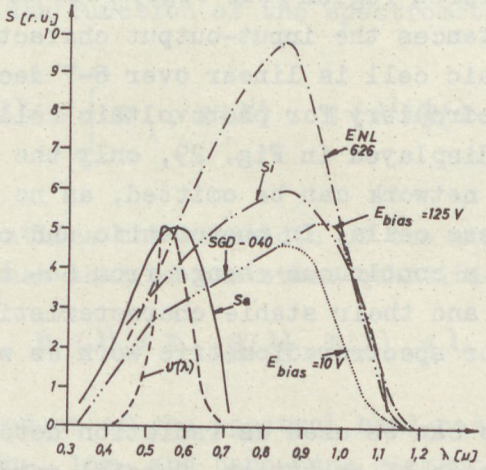

Fig. 34

Relative spectral sensitivity distribution of the human eye /$V(\lambda)$ /, of a Se-photovoltaic cell /Se/, Si-photovoltaic cell /Si/ and Si-photodiodes /SGD-040 and ENL 626/

Drawbacks of the Se-cell are the following: Quite considerable fatigue for both high and low levels of irradiation, which is in some cases even spectrally selective; non-linearity of light intensity versus output current: for medium and strong illumination the linearity holds, if used in short circuit circumstances; for currents under 1 μA, however, even cells of the best types show non-linearities,

hysterezys and inconsistent readings. The sensitivity of Se-cells, as high as 5-600 μA/lm is usually not constant along the cell surface, producing sometimes measuring difficulties. The enumerated drawbacks exclude them almost entirely from the use in spectrometric measurements.

The more recent p-n junction Si photovoltaic cells, on the other hand, do not suffer from these drawbacks. They are highly stable, sensitive receivers, the spectral sensitivity of which extends over the entire visible spectrum into the near infrared region /see Fig.34/. If used under short circuit circumstances the input-output characteristics of a Si photovoltaic cell is linear over 6-7 decades of illumination. The circuitry for photovoltaic cells is very similar to that displayed in Fig. 29, only the dark current compensating network can be omitted, as no dark current exists in these cells. In photometric and colorimetric measurements a continuous change from Se- to Si-cells can be observed, and their stable characteristics make them candidates for spectroradiometric work as well.

p-n junctions can be used as radiation detectors also in back-biased mode of operation. Special gard-ring constructions make high sensitivity, high frequency operation possible. These cells possess a definite dark-current, which is temperature dependent, therefore it is practical to use these detectors in a.c. circuits. Latest achievements in Si photodetector technology are the p-i-n or avalanche photodiodes. In these devices an inner amplification takes place: the voltage on the diode is chosen so high that the electrons traversing through the barrier are accelerated to such a velocity to be able to produce secondary electrons. Modern diodes possess an amplification factor of 100--1000, the cell voltages lie in the order of 100 V. These photodiodes can be used in many applications instead of photomultipliers. A detailed study of their performance characteristics /fatigue effects, long-term stability,

spectral sensitivity changes, etc./ is, however, still lacking.

7. Spectrometric measurement and apparatus [21]

A spectrometric signal is a convolution of the product of the spectral power distribution function (E_λ), the transmission /or reflexion/ characteristics of the optical system $T(\lambda)$, the spectral sensitivity distribution of the receiver $S(\lambda)$ and the bandwidth function of the spectrometer $\phi(\lambda)$.

$$M(\lambda) = \int_0^\infty E_\lambda, \; S(\lambda') \quad T(\lambda')\phi(\lambda-\lambda')\,d\lambda' \qquad 38$$

In most applications the bandwidth of the monochromator is much smaller than that of the other quantities in Equ. 38, so that

$$M(\lambda) \approx E_\lambda \; S(\lambda) \; T(\lambda) \; d\lambda \qquad 39$$

$T(\lambda)$ is the product of the spectral band-pass characteristics of several high-, low- and band-pass elements: thus, for instance, the absorption of the dispersion element, the spectral reflexion and absorption of the mirrors and the lenses in the light way and the transmission $\tau(\lambda)$ /or reflexion $\varrho(\lambda)$/ characteristics of the sample:

$$T(\lambda) = T_1(\lambda) \ldots T_n(\lambda)\,\tau(\lambda)\,\varrho(\lambda) = T'(\lambda)\,\tau(\lambda)\,\varrho(\lambda) \qquad 40$$

The purpose of the spectrometric measurement is the determination of either E_λ or $S(\lambda)$ or $\tau(\lambda)$ or $\varrho(\lambda)$. In case of $\tau(\lambda)$ measurement the situation is relatively simple. By the help of two measurements with and without the sample in the light way

$$M^{\sim}(\lambda) = E_\lambda \quad S(\lambda)\,T'(\lambda)\,\tau(\lambda)$$

$$M^{o}(\lambda) = E_\lambda \quad S(\lambda)\,T'(\lambda)$$

the desired quantity can be directly obtained as

$$\tau(\lambda) = \frac{M^{\tau}(\lambda)}{M^{o}(\lambda)} \qquad 41$$

This is the method in normal spectrophotometric practice. In case of reflexion, power distribution and sensitivity determinations, however, this direct method cannot be used: without light source and receiver no measurement can be performed. Also the diffuse reflectance has to be measured compared with the perfect diffuser, the realization of which is rather cumbersome. Thus in all these cases the measurements are carried out by comparing the unknown E^{x}_{λ}, $S^{x}(\lambda)$, $\varrho^{x}(\lambda)$ quantities with standard values.

The two readings are

$$M^{x}(\lambda) = E^{x}_{\lambda}\, S(\lambda)\, T(\lambda)\, d\lambda \qquad 42$$

$$M^{e}(\lambda) = E^{e}_{\lambda}\, S(\lambda)\, T(\lambda)\, d\lambda$$

and so

$$E^{x}_{\lambda} = E^{e}_{\lambda}\, \frac{M^{x}(\lambda)}{M^{e}(\lambda)} \qquad 43$$

Similar expressions can be formed for $S^{x}(\lambda)$ and $\varrho^{x}(\lambda)$.

In all these cases the unknown quantity is obtained by multiplying the ratio of two measured quantities with a prescribed value. The wavelength dependence of this "standard" has to be determined separately by comparing this working standard to a primary one /in case of the radiation source to a blackbody, for the receiver to a cavity type receiver, for the reemission standard to a perfect diffuser/. Nevertheless, for all these standard values it is true that within the limit of the stability of the standard they can be tabulated and used for repeated measurements in unchanged form.

In the following the construction of a spectrometer will be examplified for the spectral power distribution measurement.

Nevertheless, the other two types of measurements show principally nothing new.

The block diagram of a spectral power distribution measuring apparatus is to be seen in Fig. 35. The radiation of the unknown and standard light sources falls alternatively on the dispersing system /M/, the output flux of which reaches the photodetector /Ph/.

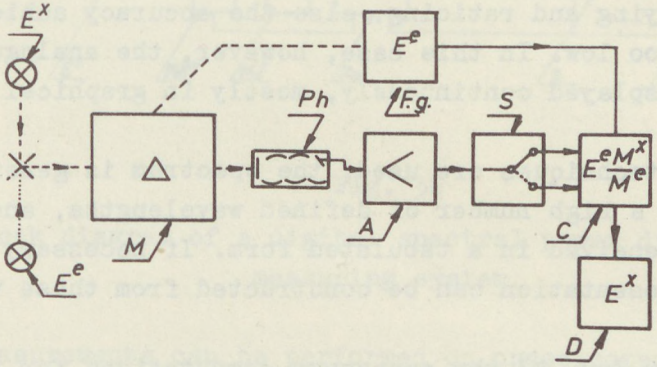

Fig. 35

Block diagram of spectral power distribution measuring procedure

In the simplest case the output of the amplifier is measured for the two sources, the tabulated value of the standard source read and the computation according to Equ. 43 performed.

In a more elaborate system real double-beam techniques can be used. The standard and unknown sources are placed into the light way alternatively, and the signals are fed into a selector /S/. According to Fig. 35 a next block, the computing one /C/ forms the ratio of the two signals and multiplies the result with the standard value that has to be synchronised to

the wavelength drum of the M dispersing-system. The function generator for E^e /Fg/ is therefore coupled to the monochromator. The result of the computation, the signal proportional to the E^x distribution is made visible on the D display unit, this might be a graphical or digital display.

The function generation has usually been built by the help of optical or electrical cam systems, tapped potentiometers or curve followers. The accuracy of all these solutions might hardly surpass 0.5 ~ 1%. Usually servo-systems have been used for multiplying and ratioing, else the accuracy achieved would have been too low. In this case, however, the analogue signal could be displayed continuously, mostly in graphical form.

If digital techniques are used, the spectrum is generally measured at a high number of defined wavelengths, and the result is received in a tabulated form. If necessary a graphical representation can be constructed from these values.

As seen from Equ. 43 the necessary computations for achieving E^x_λ are rather simple. Taking into consideration that the single measurement points follow each other rather slowly /1-10 points/min/, due to the necessary integrating time of the detecting system, three solutions of the problem seem to come into question: time-sharing work on a big computer, storing the measured signals on punched or magnetic cards or tape and performing the computation later on a central computer or building a small one-purpose equipment. In the Research Institute for Technical Physics of the Hungarian Academy of Sciences, Budapest, this third solution was chosen.

The main parts of the equipment, partly still under construction, enabling us to measure spectral power distributions, sensitivity distributions, transmission and reflexion spectra with a high accuracy, are a Hilger double monochromator /D 284/ and an EMG Hunor electronic desk calculator. The block-

diagram of the spectral power distribution measuring system is shown in Fig. 36.

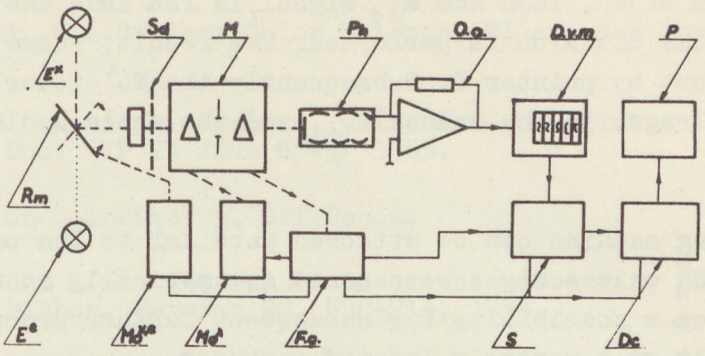

Fig. 36

Block diagram of a digital spectral power distribution measuring system

The measurements can be performed on preselected wavelengths. The wavelength drum of the monochromator is coupled with a cog-wheel carrying a 16 mm perforated movie-film. A small lamp and photocell reads the wavelength marks scratched on this filmtape. Due to the photocell signal a magnetic clutch stops the movement of the wavelength drum. Then at this fixed wavelength the measurement is performed. For this purpose, in case of spectral power distribution measurements, the wavelength setting signal starts the punched tape reading device and reads the real power distribution $E^{e}_{\lambda\ i}$ values into the Hunor desk calculator /D.c./ through the selector /S/. The rotable mirror /R.m./ turns into the position E^{x}. The light flux of the unknown lamp reaches now the photoelectric multiplier /Ph/ through the monochromator. The multiplier signal is amplified by an operational-amplifier /O.a/, the output signal of which is fed into the auto-ranging digital voltmeter /D.v.m./ EMG Type 1362. The decimally coded output of the voltmeter reaches the calculator through the selector and the

calculator multiplies the previously inscribed $E^{e}_{\lambda i}$ value with this $M^{x}_{\lambda_i}$ value. Thereafter the function generator triggers the $Mo^{x,e}$ block and this turns the rotatable mirror in the direction of E^{e}. Then the $M^{e}_{\lambda i}$ signal is fed into the calculator and the division is performed. The result, value $E^{x}_{\lambda i}$ is printed out by printer P. Subsequently the Mo^{λ} motor changes the wavelength to the value λ_{i+1} and the whole cycle starts anew.

A punching machine can be attached parallel to the printer and the E^{x}_{λ} values might be punched automatically on a tape. This gives a possibility for subsequent further processing the result on a remotely located computer.

8. SUMMARY

In the preceding sections we tried to sum up some problems and their solution one is usually confronted in spectrometric measurements. Questions related with the different standard and excitation radiation sources, methods of monochromatization, detectors and spectrometer systems have been discussed.

Spectrometric measurements are often regarded as complicated, with a lot of uncertainity and uncontrollable causes of errors. If, however, some attention is paid to the single building blocks of a spectrometric measurement and the occurring errors are systematically eliminated, it is possible to increase the reproduction accuracy of a spectrometric measurement to better than $\pm$ 0.2 ~ 0.5%, and the absolute precision, too, within several per cents.

L I T E R A T U R E

1. G.Wyszecki, W.S.Stiles: Color Science, Wiley, New York, 1967.

2. IUPAP-SUN Commision: Symbols, units and nomenclature in physics. Doc. UIP II /Sun 65-3/ 1965.

3. CIE Doc. on Colorimetry. Off.Recom.

4. J.C. de Vos: A new determination of the emissivity of tungsten ribbon. Physica 20, 690-714, 1954.

5. G.A.W.Rutgers, K.Schurer: Radiation Standards. 4th IMEKO-Symp. on Photon-Detectors. Prague, 1969. Ed.M.Jedlička, Telsa-Vúvet. Prague, 1970. p.225-34.

6. G.A.W.Rutgers, J.C.de Vos: Relation between brightness temperature, true temperature and colour temperature of tungsten. Luminance of tungsten. Physica 20, 715-20,1954.

7. J.Schanda: A spektrális teljesitményeloszlás mérésénél fellépő hibák elemzése. Magy.Fiz.F. 10, 455-77. 1962.

8. M.Neumann: Betriebsgesetze der Halogenglühlampe. Lichttechnik 2/16, 63A-65A. 1969.

9. J.Schanda, G.Szigeti: Stability of high colour temperature etalon lamps. CIE XVII. Congr. Barcelona, 1971.

10. F.Rössler: Quecksilberhochdrucklampe, Ann.d.Phys. 34, 1. 1939.

11. Hanau Quarzlampen Ges.m.b.H. Catalogue.

12. G.Bauer: Strahlungsmessung im optischen Spektralbereich, Vieweg, Braunschweig, 1962.

13. R.L.Aspden: Electronic flash photography. Macmillan, New York, 1960.

14. K.S.Gibson: Spectrophotometry, NBS Circ. 484. 1949.

15. Zeiss, Jena: SPM-2 Monochromator manuel.

16. W.E.K.Middleton, C.L.Sanders: The absolute spectral diffuse reflectance of magnesium oxide. J.Opt.Soc.Am. 41, 419. 1951.

17. C.L.Sanders, W.E.K.Middleton: The absolute spectral diffuse reflectance of magnesium oxide in the near infrared. J.Opt.Soc.Am. 43, 58. 1953.

18. J.H.Kaufhold: Zur experimentellen Bestimmung der Empfänger für den optischen Spektralbereich. Proc. 5th IMEKO Symp. on Photon-Detectors, Varna, 1971. Ed. J.Schanda. IMEKO-Secr. Budapest, 1971.

19. J.Schanda: Időbontó mikrospektrométer és alkalmazása az elektrolumineszcencia vizsgálatában. Kand.értekezés. Bp. 1967.

20. G.Eppeldauer, J.Schanda: A sensitive filter fluorimeter. J.Phys.E: Scientific Instruments 5 1197 . 1972.

21. J.Schanda: On the digital measurement of spectrometric quantities. IMEKO-Kongr. Versailles, 1970. HU-234.

x x x

ELECTROSTATIC ENERGY IN ABRUPT SEMICONDUCTOR HETEROJUNCTIONS

By
Imre Markó

1. Introduction

The equilibrium energy-band diagrams of heterojunctions have been proposed by Anderson, Oldham and Milnes and by Van Ruyven.

Anderson's model [1] can be satisfactoraly applied when the difference between the lattice constants and heat expansion coefficients of materials forming the heterojunction is so slight that interface states can not develop at the interface.

The interface states are taken into consideration by Oldham's model [2]. A further generalization was made by Van Ruyven [3,4] supposing the existance of a dipole layer in addition to the monopole layer at the interface.

All three models of the isotype heterojunction were proved for n-n heterojunctions with the added remark that probably an analogous situation arises in the p-p case. It has been found [5, 11, 12] that the effects easily measurable on n-n samples are absent on p-p ones. Opdorp and Kanerva [6,7] assume the validity of the double depletion layer model, proposed by Oldham and Milnes, and determined the discontinuity of the conduction band ΔE_c at the interface by the I - V and C - V characteristics of n-n Ge-Si samples prepared by alloying. They found that without regard to the impurity concentration in Ge and Si, ΔE_c is equal to the difference of the electron affinites of materials $\Delta \chi$. The p-p heterojunctions, all of wich were made by alloying, were invariable ohmic. The double saturation tendency of the I-V chatacteristics of the p-p Ge-Si heterojunctions were observed by Gutai, Pfeifer and Markó [6] on the samples prepared by vacuum evaporation. Gutai

and coworkers demonstrated the existence of a dipole layer on the interface by using Opdorp and Kanerva's method.

Calculation of the minimum of the free energy of the system might provide the theoretical foundation for the choice of the suitable model. The electrostatic energy is a very important component of the free energy. In agreement with Frankl /8/ we suppose a dependence of the electrostatic energy upon only those parameters of wich the other terms in the expression of free energy are independent, so that the minimum of free energy shall coincide with the minimum of electrostatic energy.

2. Electrostatic energy

In order to be able to determine the changes of the macropotential, ϕ let us consider the electrostatic energy which accumulates at the semiconductor heterojunction. In the general case, when the lattice constant of materials forming the heterojunction differ, the interface states will capture electric charges and a surface monopole layer will develop. Thus we may consider a model in which two cemiconductors of different materials, each bounded by a plane face, are approached to an electrically charged plate without thickness and possessing a surface charge /monopole layer/ Q untill complete contact. At the moment of the contact the electrostatic energy will have a minimum value and the space charges in the two semiconductors will compensate the electric charge of the plate:

$$Q_1 + Q_2 + Q = 0 \qquad /1/$$

where Q_1 and Q_2 are the accumulated charges in the space charge region of semiconductors of unit surface. Let us now find the minimum of the electrostatic energy related to the unit area of the surface:

$$W = 1/2 \int E/x/\ D/x/\ dx \qquad /2/$$

where x is the coordinate axis in the direction perpendicular to the interface.

Using the depletion layer approximation the condition of neutrality [1] can be written in the form:

$$\left(\frac{kT}{2\pi}\right)^{1/2}\left(\sqrt{\varepsilon_1 \rho_1 \psi_2} + \sqrt{\varepsilon_2 \rho_2 \psi_2}\right) + Q = 0 \qquad /3/$$

where ρ_1 and ρ_2 are the electric charge carrier's concentrations, ε_1 and ε_2 are the dielectric constants of the component materials of heterojunction respectively, e is the electric charge of electron, k the Boltzman constant, T the absolute temperature, and

$$\psi = \frac{\varphi}{kT}$$

where φ is the electrostatic potential satisfying the Poisson equation.

The electrostatic energy of this structure can be written as

$$W = (8\pi)^{1/2}\left(\frac{kT}{3e}\right)^{3/2}\left(\sqrt{\varepsilon_1 \rho_1}\,\psi_1^{3/2} + \sqrt{\varepsilon_2 \rho_2}\,\psi_2^{3/2}\right) \qquad /4/$$

Taking the value of Q as constant, equation /3/ determines the relationship between ψ_2 and ψ_1. By making use of this relationship the derivative of equation /4/ according to ψ_1 is formed and if this derivative is equal to zero it will be possible to determine the values of ψ_1 and ψ_2 at wicht the energy in equation /4/ will have a minimum value. It can be easily proved that the condition

$$\psi_{o1} = \psi_{o2} = \psi_o . \qquad /5/$$

ensures this minimum. It should be noted that the result expressed in equation /5/ is obtained when not the complete depletion approach is used, but the exact values [13]:

$Q_1 = 2en_{i1}L_1F/\psi_{o1}; \gamma_1/$ and $Q_2 = 2en_{i2}L_2F/\psi_{o2}; \gamma_2/$ are substituted into equation /1/ and the minimum of the expression

$$W = \left(\frac{kT}{e}\right)^2\left[\frac{\varepsilon_1}{2L_1}\int_0^{\psi_{o1}} F(\psi_1;\gamma_1)\,d\psi_1 + \frac{\varepsilon_2}{2L_2}\int_0^{\psi_{o2}} F(\psi_2;\gamma_2)\right] \qquad /6/$$

is sought. Equation /6/ can be derived on the ground of cite/8/ where n_{i1} and n_{i2} are the intrinsic concentrations in the materials,

$$L = \left(\frac{kT\,\mathcal{E}}{8\pi e^2 n_i} \right)^{1/2} ; \quad \gamma = n/n_i = n_i/p,$$

n and p is the actual concentration of the electrons and holes, respectively.

$$F(\psi, \gamma) = \left[\gamma(e^{-\psi} - 1) + \gamma^{-1}(e^{\psi} - 1) + \psi(\gamma - \gamma^{-1}) \right]^{1/2}$$

Since $\psi_o = V_D/kT$, the electrostatic energy is minimum when the diffusion potentials are the same in the two materials. This illustrated in Fig.1

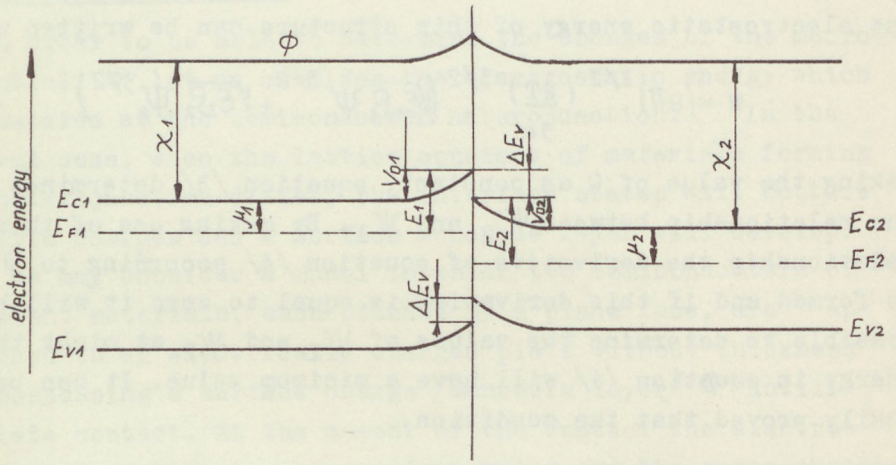

Fig.1.

Schematic non-equilibrium energy-band diagram of an n-n heterojunction at the moment of the contact.

However, the state which has developed in this way is not a steady-state condition, since due to the gradient of the Fermi level transport processes begin in the sample. In case of equilibrium $E_{F1} = E_{F2}$, which means that either the condition of minimum electrostatic energy or that of the continuity of the macropotential ϕ has to be abandoned. Next

the separate consequences of the two conditions will be scrutinized from the energy aspect.

a. ϕ shall be continuous and E_F = const.
In this case:

$$\psi_{01} = \frac{\Delta\chi}{kT} + \frac{\Delta\mu}{kT} + \psi_{02} \qquad /7/$$

where $\Delta\chi = \chi_2 - \chi$ and $\Delta\mu = \mu_2 - \mu_1$
For a given pair of materials $\Delta\chi$ is constant and $\Delta\mu$ depends on the bulk concentration of the components, which in a concrete case may also be considered as constant.
Thus $\psi_{01} = \psi_{02}$ + const and

$$W = \sqrt{8\pi}\,\frac{(kT)^{3/2}}{3e}\left(\sqrt{\rho_1\varepsilon_1}\,\psi_{01}^{3/2} + \sqrt{\rho_2\varepsilon_2}\,(\psi_{01}+C)^{3/2}\right) \qquad /8/$$

b. In the second case E_F= const, W = minimum and Q shall still be considered as constant. In this case a dipole layer of ν dipole density is incorporated into the interface causing a jump

$$\nu = \sigma d = \frac{\Delta\chi + \Delta\mu + kT(\psi_{02}-\psi_{01})}{e}$$

in the potential, and giving an additional term to the energy expression /4/:

$$W = \sqrt{8\pi}\,\frac{(kT)^{3/2}}{3e}\left[\sqrt{\varepsilon_1\rho_1}\,\psi_{01}^{3/2} + \sqrt{\varepsilon_2\rho_2}\,\psi^{3/2}\right] + \frac{\sigma}{e}\left[C + kT(\psi_{01}-\psi_{02})\right] \qquad /9/$$

Still assuming that in equation /1/ Q is constant, we obtain a correlation between ψ_{01} and ψ_{02}. Minimalization of equation /9/ leads to a correlation between σ and the diffusion potentials. Differentiating the energy expression /9/ with regard to ψ_1, and making it equal to zero, σ can be expressed in the following manner:

$$\sigma = \frac{\sqrt{8\pi kT\varepsilon_1\varepsilon_2\rho_1\rho_2}\,(\psi_{01}-\psi_{02})}{3(\sqrt{\varepsilon_1\rho_1}\,\psi_{02} + \sqrt{\varepsilon_2\rho_2}\,\psi_{01})} \qquad /10/$$

It appears that the dipole layer changes the minimum condition equation /5/. The deviation can be written as

$$\psi_{01} = \psi_0 - \Delta_1 \qquad /11/a/$$

$$\psi_{02} = \psi_0 - \Delta_2 \qquad /11/b/$$

Let ψ_0 be defined as

$$\psi_0 = \frac{2\pi}{kT} \frac{Q^2}{(\sqrt{\varepsilon_1 \rho_1} + \sqrt{\varepsilon_2 \rho_2})^2} \qquad /12/$$

If compared to ψ_0 Δ, and Δ_2 are small, $\psi_{01}^{1/2}$; $\psi_{02}^{1/2}$; $\psi_{01}^{3/2}$ and $\psi_{02}^{3/2}$ can be expanded into a series of ascending power of Δ_1 and Δ_2, respectively. Taking into consideration equations /11a/,/11b/ and /12/ the following correlation is obtained between Δ_1 and Δ_2, neglecting the second and higher order terms in /3/:

$$\sqrt{\frac{\varepsilon_1 \rho}{\varepsilon_2 \rho_2}}\, \Delta_1 = \Delta_2 \qquad /13/$$

On ground of the above σ can be expressed as a function of Δ_1:

$$\sigma = \frac{\sqrt{8\pi kT \varepsilon_1 \varepsilon_2 \rho_1 \rho_2}\ \left(1 + \sqrt{\frac{\varepsilon_1 \rho_1}{\varepsilon_2 \rho_2}}\right) \Delta_1}{3\left[(\sqrt{\varepsilon_2 \rho_1} + \sqrt{\varepsilon_2 \rho_2})\sqrt{\psi_0} + \frac{\Delta_1}{2\sqrt{\psi_0}}\left(\sqrt{\varepsilon_1 \rho_1} + \frac{\varepsilon_1 \rho_1}{\sqrt{\varepsilon_2 \rho_2}}\right)\right]} \qquad /14/$$

In the denominator of equation /14/ compared to the first the second term can be neglected. Using equation /12/ an approcimation is obtained for σ:

$$\sigma = \frac{kT \sqrt{\varepsilon_1 \varepsilon_2 \rho_1 \rho_2}\ \left(1 + \sqrt{\frac{\varepsilon_1 \rho_1}{\varepsilon_2 \rho_2}}\right)}{Q} \Delta_1 \qquad /15/$$

Substitution of equations /11a/, /11b/, /12/ and /13/ into equation /9/ leads to an approximate expression of the energy which can be assigned to charge Q in the heterojunction, as a function of the parameter Δ_1. When seeking the minimum

of the energy obtained in this manner we arrive at the following value:

$$\Delta_1 = \frac{\Delta\chi + \Delta\mu}{3kT\left(1+\sqrt{\frac{\varepsilon_1\varrho_1}{\varepsilon_2\varrho_2}}\right)} \qquad /16/$$

It can be seen that the values of Δ_1 and Δ_2 depend exclusively on the bulk properties of the materials forming the heterojunction, while ψ_0 and ψ - as apparent from equations /12/ and /15/ - depend on the value of the charge captured by the interface states.

3. Sample preparation

The measurement were carried out on Ge-Si p-p heterojunctions. The samples were prepared in the Research Institute for Technical Physics of the Hungarian Academy of Sciences by the evaporation of Ge in ultrahigh vacuum - its condensation on single crystal Si substrate. The substrate was a Si single crystal of /111/ orientation and of 300-350 /um thickness having 200 to 300 ohmcm resistivity. The thickness of the Ge layer was 10 to 15/um. The ohmic contacts were checked by applying both to the Ge and to the Si side 2 contacts each and investigating the current and capacitive properties between contacts on the same side. With some samples evaporated Au contacts, with others Ni contacts - applied by current-free galvanization /Sullivan-Eigler method/- were used. The resistance of contacts prepared by any of the two methods was satisfactory. Due to shunt effects great difficulties were encountered when trying to determine the concentration of impurites in the layer and in the substrate. The measurement on the Schottky barrier applied to the layer and to the substrate appeared to be the most reliable method.

4. Experimental

The I-V characteristics were recorded by means of a Cimatic X-Y recorder of 10^{-4} V/cm sensitivity. Low currents were measured with the Unipan 219 electrometer. The samples were immersed in paraffin oil or placed into ampoules evacuated

to 10^{-4} Torr pressure. Samples prepared by the different method gave the same results.

The I-V characteristics show a double saturation tendency which enabled the use of the evaluation method suggested by Opdorp and Kanerva [5, 7]. In our case, however, using the symbols of Ref. [5,7], it was not possible to apply the $I_{s2} \gg I_{s1}$ approcimation, since experiments showed that the saturation currents /I_{s1} and I_{s2}/ were of the same order. For this reason the more exact formulas

$$I_{s1} = \frac{2kT}{eR_o}\left(1 \mp \sqrt{1 - R_o/R_{oo}}\right) \qquad /17/a/$$

$$I_{s2} = \frac{2kT}{eR_o}\left(1 \pm \sqrt{1 - R_o/R_{oo}}\right) \qquad /17/b/$$

were used, where R_o is the value of the differential resistance in the inflexion point of the I-V characteristic,while R_{oo} is the differential resistance in the origin. Accordingly, the values of E_1 and E_2 were determined from the slopes of the curves

$$-k \ln\left[\frac{1 - \sqrt{1 - R_o/R_{oo}}}{R_o T}\right] \quad \text{vs} \quad \frac{1}{T}$$

and

$$-k \ln\left[\frac{1 + \sqrt{1 - R_o/R_{oo}}}{R_o T}\right] \quad \text{vs} \quad \frac{1}{T}$$

$$E_1 = \mu_1 + kT(\Psi_0 - \Delta_1) \qquad /18/a/$$

$$E_2 = \mu_2 + kT(\Psi_0 + \Delta_2) \qquad /18/b/$$

With the help of equations /10/, /11/ and /12/ the charge density σ responsible for the dipole layer can also be determined. It should be noted that if the condition $\psi_0 \gg \Delta_1$ and $\psi_0 \gg \Delta_2$ is fulfilled, $E_2 - E_1 = \Delta\mu$.

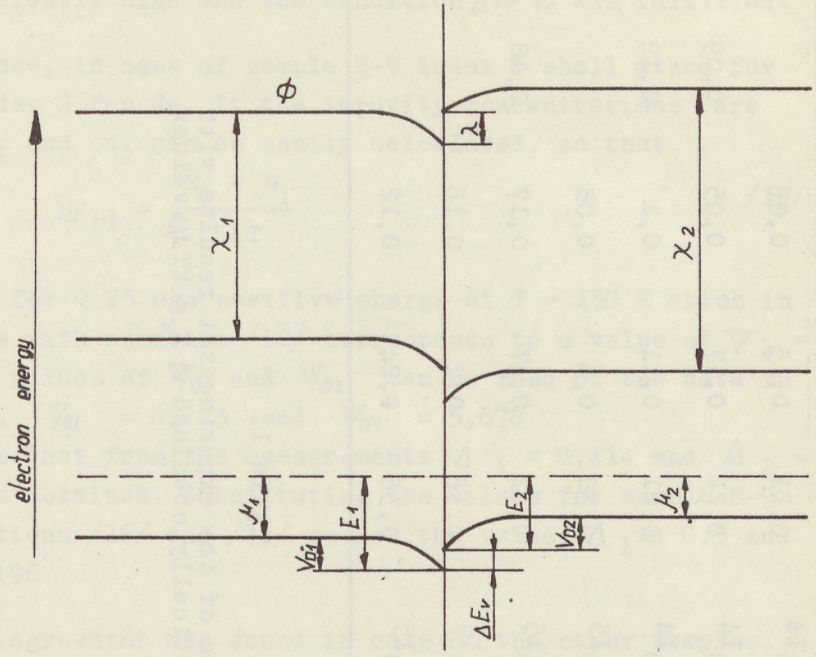

Fig. 2.
Equilibrium energy-band diagram of p-p heterojunction

The experimental results are summed up in the following Table:

Sample	$P_{Si}[cm^{-3}]$	$P_{Ge}[cm^{-3}]$	E_{Si} [eV]	E_{Ge} [eV]	ΔE_V [I-V]	ΔE_V (C-V)	$\Delta E_V = kT$	$(\mu_2-\mu_1)$
C-17/4	10^{14}	3.10^{14}	0,21	0,15	0,06		0,06	T=150K
C-17/6	10^{14}	$5,10^{14}$	0,22	0,17	0,05	0,09	0,07	T=150K
C-17/10	7.10^{13}	$5,10^{14}$	0,21	0,11	0,1	0,12	0,10	T=150K
H-9	2.10^{14}	10^{15}	0,38	0,3	0,08		0,06	T=150K
H-14	10^{14}	3.10^{15}	0,64	0,47	0,17	0,18	0,15	T=300K
H-14/a	10^{14}	3.10^{15}	0,36	0,2	0,16		0,15	T=300K
H-14/d	10^{14}	3.10^{15}	0,36	0,24	0,12		0,15	T=300K

Table 1.

Comparasion of the experimental results with the theoretically obtained $\Delta E_V = kT\Delta/\mu$ values

5. Results and conclusions

It appers from Table 1.that it is impossible to interpret the experimental results on ground of the arguments presented in par. 2a, while the approximating formulas in par 2b show good agreement with experimental result.It should, however be emphasised that in our samples the interface charge was sufficiently high and the condition $\Delta \ll \Psi_0$ was fulfilled.

For instance, in case of sample H-9 index 1 shall stand for Si and index 2 for Ge. It the impurity concentrations are known, $/u_1$ and $/u_2$ can be easily calculated, so that

$$\Psi_{oi} = \frac{E_i - \mu_i}{kT} \qquad /19/$$

We obtain for Q 25 cgs positive charge at T = 150 K which in accordance with equation /12/ corresponds to a value of Ψ_0 = = 6,1 The values of Ψ_{01} and Ψ_{02} can be read of the data in the Table. (Ψ_{02} = 6,273 and Ψ_{01} = 5,678
This means that from the measurements Δ_1 = 0,414 and Δ_2 = = 0,173 is obtained. Substituting the values for sample H-9 into equations /16/ and /13/ we get the values $\Delta_1 \approx 0{,}5$ and $\Delta_2 \approx 0{,}198$

A similar agreement was found in case of the other samples. The experimentally determined Δ_1 and Δ_2 values are all - as expected - lower than the values calculated from the approximating equation /16/, but the deviation is always below 15%.

It follows from the above that in case of heterojunctions it is generally appropriate to draw conclusions with respect to changes in potential on the interface from the condition W = min. Moreower it was seen that supposing the continuity of ϕ - which was made by others [2; 7] - a result was yielded agreeing with the above in the only case when.

6. Acknowledgment

The author wishes to thank L. Gutai and T. Vicsek for several helpful discussions concerning this article.

REFERENCES

1. R.L. Anderson; Sol. Stat. Electron 5 341 /1962/
2. W.G. Oldham and A.G.Milnes; Sol.Stat,Electron 7 153/1964/
3. L.J.van Ruyven; J.M.P. Papenhuyzen and H.C.J.Ver Jocuen: Sol.Stat.Electron 8 631 /1965/
4. L.J.van Ruyven; Phys.stat.sol. 3 K109 /1964/
5. G.van Opdorp; Philips Res. Rept. Suppl. 1969, N° 10
6. L.Gutai, J.Pfeifer, I.Markó; Proc. of the Int. Conf. on the Phys. and Chem. of Semiconductor Heterojunctions and Layers Structures, Vol II. p 301.
7. G.van Opdorp and H.K.J.Kanerva; Sol.Stat.Electron 10 401 /1967/
8. D.R.Frankl; Surface Science 9 73 /1968/
9. Г.Е.Пикус; Основы теории полупроводниковых приборов Москва 1965
10. I.Markó; Thesis, Szeged 1972
11. R.L.Anderson; U.S.Defence Report AD 635026, Clearinghouse p.172/1966./
12. J.Brownson; J.Appl.Phys. 35 1356 /1964/
13. R.H.Kingston and S.F.Neustadler; JAP.26 718 /1955/

On the minority carrier lifetime anisotropy in plastically deformed p-type germanium

By

I.Cseh and B.Pődör

Research Institute for Technical Physics of the Hungarian Academy of Sciences, Budapest

Dislocations generated by plastic deformation exert a strong influence on the electrical properties of semiconductor crystals. In germanium the electrical transport effects /carrier mobility, magnetoresistance, electrical conductivity etc./ show a pronounced anisotropy due to the dislocations, [1, 2]. The aim of the present study was to investigate the photoelectric effects and minority carrier lifetime in plastically deformed p-type germanium. Only a short account of the most important results is given, more details are published elsewhere [3].

Photoconductivity /PC/ and photomagnetoelectric effect /PME/ were measured on p-type samples of plastically bent germanium between 100 and 300 K temperature. The room temperature resistivity of the samples was 20-25 ohmcm, the bent in dislocation density was about 5×10^{6}-1×10^{7} cm^{-2}, with most of the dislocations lying parallel to the bending axis [1,3].

After bending or heat treatment, double-cross-type Hall bars were cut out from the samples, so that their long axis was either perpendicular or parallel to the bending axis. The samples were etched in hot H_2O_2 and their non-illuminated lower part was mechanically polished. The potential arms and the end contacts were properly shaded. The samples were illuminated with rectangular white light pulses at an intensity corresponding to a rate of electron-hole generation of the order of 10^{16} cm^{-3} sec^{-1}. The steady state PC and the PME

open-circuit voltage were measured by a selective microvoltmeter at 37.5 Hz; the magnetic field was 3 kG. Fromt the measured PME and PC voltages the so-called "ratio lifetime" of the minority carriers was deduced.

Hall effect and electrical conductivity were measured between 77 and 300 K on the same samples [3].

The lifetime of the minority carriers before bending at room temperature was several. hundred /usec. Heat treatment did not change this value appreciably, but after bending the lifetime decreased to 1 /usec or less. The temperature dependence of the lifetime in a bent crystal is shown in Fig. 1. The striking feature is the strong anisotropy of the lifetime depending on the mutual direction of dislocations and current flow. The forms of the curves are similar but the lifetimes measured with the current parallel or perpendicular to the dislocations differ by about one order of magnitude.The diffusion coefficient of the minority carriers i. of the electrons was assumed to be isotropic, as is usual in

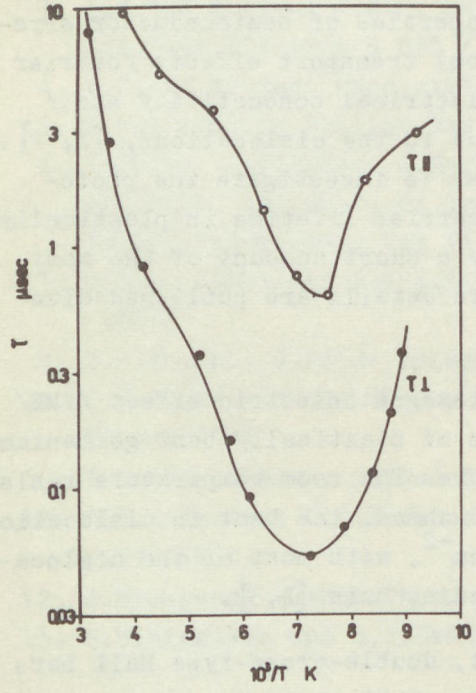

Fig.1.

Lifetime vs. reciprocal temperature in plastically deformed p-type Ge crystal. Lifetime: $\tau_{\parallel}$ - measured parallel to the dislocations, $\tau_{\perp}$ - measured perpendicularly to the dislocations.

converting the measured data to lifetimes [3,4]. The validity of this assumption /see e.g.[4]/ will be discussed later.

In spite of the relatively high generation rate used in our experiments the lifetime vs temperatura curves clearly displayed the recombination and trapping range, in a qualitative agreement with the results of [5]. Although the high generation rate makes it impossible to calculate an accurate value of activation energy from the curves in the trapping range, a lower limit of 0.15-0.16 eV can be established under our experimental conditions. These values are considerably lower than those obtained in[5] for very low generation rates, but they can be considered as a lower limit for the position of a set of energy levels connected with the dislocations.

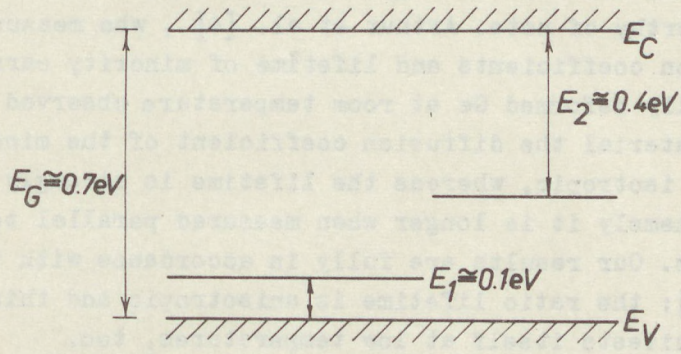

Fig. 2.
Prosped energy level scheme for dislocations in p-type germanium

In order to interpret our experimental results the following tentative energy level scheme is propesed for the dislocations [3], see Fig. 2. The first shallower level at about o.l eV above the valence band is that one observed in[6] and gives rise to donor action of dislocations at low temperatures. Our Hall effect results propably due to the reasons discussed in [6] did not show this level[3]. The second level is the one observed by one of us [1] in Hall effect measurements and by

Jastrzebska and Figielski[7] in recombination experiments, and lies about 0.4 eV below the conduction band. As it has an acceptor character, it is very easy to observe its effects in n-type Ge. However, by Hall effect measurements on p-type crytals it could be observed only if the Fermi level crossed this second one[3]. In experiments with injected carriers in p-type germanium it is this second level that is observed[5]. The injected minority carriers /i.e. electrons/ are captured by this second level and a negative charge is built up on the dislocations; these are screened by the free holes and very similarly to the case of n-type germanium, a potential barrier is developed which controls the recombination and trapping of injected carriers.

The appearence of an anisotropy in the ratio lifetime is particularly worthy of note. Arthur et al. [4] , who measured the diffusion coefficients and lifetime of minority carriers in plastically deformed Ge at room temperature observed that in p-type material the diffusion coefficient of the minority carriers is isotropic, whereas the lifetime is strongly anisotropic, namely it is longer when measured parallel to the dislocations. Our results are fully in accordance with the result of[4]; the ratio lifetime is anisotropic and this anisotropy manifests itself at low temperatures, too.
In evaluating the measurements we assumed, in line with the room-temperature measurements of Arthur et al.,[4] that the diffusion coefficient is isotropic.

A likely mechanism for the observed anisotropy of lifetime based on the original ideas of Arthur et al.[4], can be saught in terms of the presumed existence of deep-lying acceptor-like levels in p-type Ge[3]. The negative charge on this level, it appears, creates a space charge region around the dislocation which impedes the capture of minority carriers /i.e.electrons/ on the dislocations flowing perpendicularly to them.

References

1. B.Pődör, Acta Phys. Hung. 23 393 1967.
2. J.Balázs and B.Pődör, phys.stat.sol. 37 119 1970.
3. I.Cseh and B.Pődör, Acta Phys. Hung., 1973, in press.
4. J.B.Arthur, A.F.Gibson, J.W.Granville and F.G.S.Paige,Phil. Mag., 3 940 1958.
5. M.Jastrzebska and T.Figielski, phys.stat.sol. 32 791 1969.
6. W.Schröter, phys.stat.sol.21 211 1967.
7. M.Jastrzebska and T.Figielski, phys.stat.sol.14 381 1966.

BIBLIOTHECA ACADEMIAE SCIENTIARUM
MAGYAR TUDOMÁNYOS AKADÉMIA KÖNYVTÁRA
HUNGARICAE

J094